The Dissertation Committee for Kotaro Sasaki Certifies that this is the approved version of the following dissertation:

Analysis of potential muscular determinants of the preferred walk-run transition speed in human gait

Committee:

Richard R. Neptune, Supervisor

Ronald E. Barr

Benito Fernandez

Roger P. Farrar

Lawrence D. Abraham

Analysis of potential muscular determinants of the preferred walk-run transition speed in human gait

by

Kotaro Sasaki, B.S., M.A.

Dissertation

Presented to the Faculty of the Graduate School of

The University of Texas at Austin

in Partial Fulfillment

of the Requirements

for the Degree of

Doctor of Philosophy

The University of Texas at Austin

August, 2004

Dedication

I dedicate this dissertation to my parents, Mizuho and Sadao Sasaki.

Acknowledgements

First of all, I thank Heavenly Father for all power, wisdom and guidance that He gave me to complete this work. To my advisor, Dr. Richard Neptune, I thank you for your enthusiastic advice, encouragement, kindness and support. To my brothers in Christ, Eric Schneider, Kirby Barker, Tom and Alice Abbott, thank you for your friendship and prayer. To people who proofread my dissertation, Martin Poenie, Elizabeth Nacozy, Evan Goldberg and Rob Zmitrewicz (and of course, Dr. Neptune), thank you for your time and kindness. Finally, I thank all of my family members who have continuously encouraged and supported me.

Analysis of potential muscular determinants of the preferred walk-run transition speed in human gait

Publication No._____

Kotaro Sasaki, Ph.D.

The University of Texas at Austin, 2004

Supervisor: Richard R. Neptune

The spontaneous transition from walking to running as walking speed increases is an intriguing neuromotor phenomenon that consistently occurs near 2 m/s in humans. Despite investigations of various metabolic and biomechanical factors, the determinants of the transition have remained elusive. However, no study has investigated the potential influence of intrinsic muscle properties and fiber-tendon interactions as potential determinants. The overall objective of this research was to use a forward dynamical simulation framework in three studies to identify the potential influence of these muscular determinants on the preferred walk-run transition speed (PTS).

In the first study, individual muscle force production was examined as walking speed increased to assess the influence of intrinsic muscle properties on the PTS. The simulation data showed that of all the major lower-extremity muscle groups examined, the ankle plantar flexors were the only muscles to show a decrease in force production, despite an increase in activation, as walking speed approached the PTS. The force reduction was attributed to adverse contractile conditions. Considering the importance of

the plantar flexors to providing body support and forward progression, the impaired force generation was deemed an important determinant of the PTS.

In the second study, individual muscle contributions to body support and forward progression in walking and running at the PTS were quantified to clarify differences in muscle function between the two gait modes. The most distinctive difference was the reduced soleus contribution to forward progression in running. All other muscle groups performed similarly between the two gait modes.

In the third study, individual muscle fiber and tendon mechanical work was quantified to examine whether there existed an energetic advantage during walking and running above and below the PTS. The total muscle fiber work was found to be higher in running than walking below the PTS, and higher in walking than running above the PTS. In addition, tendon elasticity utilization was lower in running below the PTS than in running above the PTS. These results highlight the advantages of each gait mode and suggest why walking below the PTS and running above the PTS are the preferred gaits.

Table of Contents

List of Tables

List of Figures

INTRODUCTION

A comprehensive understanding of how individual muscles contribute to the task requirements in gait is essential to gain insight into neuromotor control strategies used in human locomotion. Identifying the biomechanical functions of individual muscles to perform a given locomotor task in healthy individuals can also serve as a basis for comparison with impaired populations. Such comparisons are important to elucidate neuromotor disorders in impaired patient populations and establish objective scientific evidence for designing effective rehabilitation strategies.

Walking and running are the two most common modes of gait used in human locomotion, with each mode more suitable than the other depending on the speed of locomotion. An intriguing phenomenon in human gait is the spontaneous transition between walking and running, which occurs near 2 m/s (e.g., Thorstensson and Roberthson, 1987). This preferred transition speed (PTS) is consistent regardless of age, gender or anthropometric dimensions (e.g., Hanna et al., 2000; Hreljac, 1995a, b; Tseh et al., 2002). Identifying the determinants of this transition has been approached from various perspectives, including the investigation of several metabolic and biomechanical factors (e.g., Hreljac, 1995a; Prilutsky and Gregor, 2001; Raynor et al., 2002; Brisswalter and Mottet, 1996; Minetti et al., 1994). However, the results of these studies have been either conflicting or inconclusive. To date, no study has investigated the potential influence of intrinsic muscle properties and muscle fiber-tendon interactions as potential determinants of the gait transition. Furthermore, no study has investigated differences in the functional roles of individual muscles to achieve the necessary task requirements (e.g., body support and forward progression) between walking and running, which would

provide important insight into potentially different neuromotor control strategies associated with the gait transition.

Traditionally, analyses of human gait have relied on inverse dynamics analyses with EMG measurements to estimate a muscle's contribution to the task performance. Such analyses are limited in their ability to isolate individual muscle contributions to the body segment energetics (e.g., Zajac et al., 2002). In contrast, forward dynamic simulations provide a powerful framework for analyzing individual muscles including identifying muscles' contractile state (fiber length and velocity), force output and contributions to resulting body segment energetics and accelerations during locomotion. In recent years, this approach has been used to assess muscle function during walking at self-selected speeds (e.g., Neptune et al., 2001, 2004a, b; Zajac et al., 2003; Anderson and Pandy, 2003). The overall objective of this research was to use a similar framework in a series of three studies to identify potential muscular determinants of the preferred walk-run gait transition. The potential determinants were examined by identifying differences in muscle function between the two gait modes and the potential influence that intrinsic muscle properties and muscle fiber-tendon interactions have on the preferred walk-run transition speed.

In the first study, intrinsic muscle properties associated with the force-activation-length-velocity relationships were investigated during walking at increasing speeds to determine whether any particular muscle groups were over-exerted (i.e., reduced muscle force production despite increased muscle activity) at higher speeds. Previous EMG-based analyses have suggested that several swing-phase muscles are activated near maximally during walking near the PTS, and therefore serve to initiate the transition from walking to running (e.g., Hreljac, 2001; Prilutsky and Gregor, 2001). However, muscle activity alone provides little information about the capacity of a muscle to produce force.

The muscle's contractile state may be more indicative of whether a muscle's force generation is impeded or has reached its maximum capacity at higher walking speeds. A specific hypothesis examined was that the force output in the ankle plantar flexors is impaired due to intrinsic muscle properties at the PTS, and thus serves as an important determinant for the walk-to-run transition since the muscles are the primary contributors to body support and forward progression during late stance in walking (Neptune et al., 2001).

In the second study, individual muscle contributions to body support and forward progression were quantified in walking and running at the PTS to investigate differences in muscle function in the two different gait modes at the same speed. Although contributions to the task requirements in walking at self-selected speeds have previously been identified (Neptune et al., 2001, 2004a; Zajac et al, 2003), little is known about the functional roles of individual muscles during running at the same speeds. Identifying differences in individual muscle function during the different motor tasks would provide important insight into the muscle coordination strategies associated with the gait transition.

In the third study, mechanical work done by individual muscle fibers and tendons was quantified to examine whether there existed any advantages related to the mechanical fiber-tendon interactions during walking and running above and below the PTS. Previous studies have suggested that differences in energy saving mechanisms between walking and running may play an important role in metabolic energy expenditure and the selection of a particular gait mode at a given speed (e.g., Kram et al., 1997; Raynor et al., 2002). One hypothesis that was examined was that fiber work is lower in walking than in running below the PTS, and inversely, higher in walking than in running above the PTS.

A second hypothesis examined was that tendon elasticity utilization is more pronounced in running above the PTS than in running below the PTS.

CHAPTER 1

The ankle plantar flexors are important determinants of walk-run gait transition

INTRODUCTION

The spontaneous transition from walking to running during human gait as walking speed increases consistently occurs near 2.0 m/s (e.g., Thorstensson and Roberthson, 1987; Hreljac, 1993a). Many studies have analyzed the gait transition with the goal of gaining insight into fundamental neuromotor control principles that govern human and animal locomotion and identifying common mechanisms across species. However, the mechanisms initiating the transition appear multi-factorial and are not well understood (e.g., Hreljac, 1995a; Mercier et al., 1994; Diedrich and Warren, 1995).

The minimization of metabolic energy has been put forth as a potential determinant of the walk-run transition (e.g., Margaria et al., 1963; Mercier et al., 1994), but the majority of studies have concluded that the transition occurs before running becomes more economical (e.g., Brisswalter and Mottet, 1996; Minetti et al., 1994; Tseh et al., 2002). Other studies have shown little correlation between various anthropometrics and the preferred transition speed (PTS) (Hanna et al., 2000; Hreljac, 1995b) and have provided conflicting results regarding the role of various kinetic factors related to the ground reaction forces (GRFs) (Hreljac, 1993b; Raynor et al., 2002).

Hreljac (1995a) proposed that high levels of muscle activity in the ankle dorsiflexors due to high swing-phase ankle angular velocity at higher walking speeds serves as a transition trigger mechanism, since the maximum dorsiflexion velocity is

drastically reduced after the walk-run transition. In a subsequent study, Hreljac et al. (2001) found that the tibialis anterior peak EMG also decreased after the walk-run transition, which further supported the dorsiflexor hypothesis. Similarly, Prilutsky and Gregor (2001) examined EMG and joint moment data during the swing phase and concluded that in addition to the tibialis anterior, the rectus femoris and hamstrings are also highly activated and may serve as a gait transition mechanism. However, the muscle excitation state relative to its maximum is difficult to identify using EMG. The muscle's contractile state in relation to the force-length and force-velocity relationships may be more indicative of whether a muscle's capacity to produce force is impaired or reached its maximum at higher walking speeds.

Neptune and Sasaki (2004) recently hypothesized that the force produced in the ankle plantar flexors is near its maximum capacity due to intrinsic muscle properties at the PTS, and thus serves as a determinant for the walk-run transition. Their hypothesis was supported by data showing that the peak GRFs during the propulsion phase (~30 – 60% gait cycle), which are primarily the result of plantar flexor activity (Anderson and Pandy, 2003; Neptune et al., 2004a), begin to decrease near the PTS despite an increase in plantar flexor activity. A post-hoc analysis using a musculoskeletal model and experimental walking kinematic data was performed to determine the musculotendon velocities, which suggested that the ankle plantar flexors are indeed operating under adverse contractile conditions. However, their analysis only focused on the ankle plantar flexors and could not directly examine the muscle fiber lengths and velocities, which is essential for assessing the muscle force generating capacity. In addition, other muscle groups may also play an important role in the gait transition (e.g., Prilutsky and Gregor, 2001; Hreljac et al., 2001)

The overall goal of the present study was to examine the contractile state (i.e., muscle fiber length, velocity), activation level and force production in the major lower-extremity muscle groups using forward dynamic simulations of walking across a wide range of walking speeds including the PTS. The specific objective was to examine the hypothesis that ankle plantar flexor force production is impaired at higher walking speeds due to intrinsic muscle properties, and therefore serves as a determinant for the walk-run transition.

METHODS

1 Forward dynamic simulations

Forward dynamic simulations were generated to analyze the contractile state, activation level and force production in individual muscle groups during walking at increasing speeds relative to the PTS (60%, 80%, 100% and 120% PTS). A sagittal-plane biped musculoskeletal model was generated using SIMM (MusculoGraphics Inc.[1], Evanston, IL). The model and the equations of motion generated using SD/FAST (PTC Inc.[2], Needham, MA) were incorporated into the Dynamics Pipeline (MusculoGraphics Inc., Evanston, IL) to produce the forward dynamic simulations that emulated the experimental walking data.

1.1 Musculoskeletal model

The musculoskeletal model included a trunk (head, arms and torso combined as one segment) and right and left legs (each leg containing a femur, tibia, patella and foot) (Fig. 1.1). The model yielded nine degrees-of-freedom including hip, knee and ankle flexion and extension for both legs, and trunk horizontal and vertical translation and rotation (Neptune et al., 2001; Neptune et al., 2004a, b; Zajac et al., 2003). The knee flexion angle was used to prescribe two translational degrees-of-freedom of the tibia relative to the femur (Yamaguchi and Zajac, 1989) and the position and orientation of the patella relative to the tibia (Delp, 1990). Thirty visco-elastic elements were attached to each foot segment in order to model the contact between the foot and ground (Neptune et

[1] URL: http://www.musculographics.com/
[2] URL: http://www.ptc.com/

al., 2000). Fifteen Hill-type musculotendon actuators per leg were used to drive the model, which were combined into nine muscle groups (Fig. 1.1) with muscles within each group receiving the same excitation pattern. The muscle activation-deactivation dynamics was represented with a first-order differential equation (Raasch et al., 1997) with activation and deactivation time constants of 5 and 10 ms, respectively. Passive joint torques representing ligaments and other connective tissues were used to limit abnormal joint range of motion (Davy and Audu, 1987).

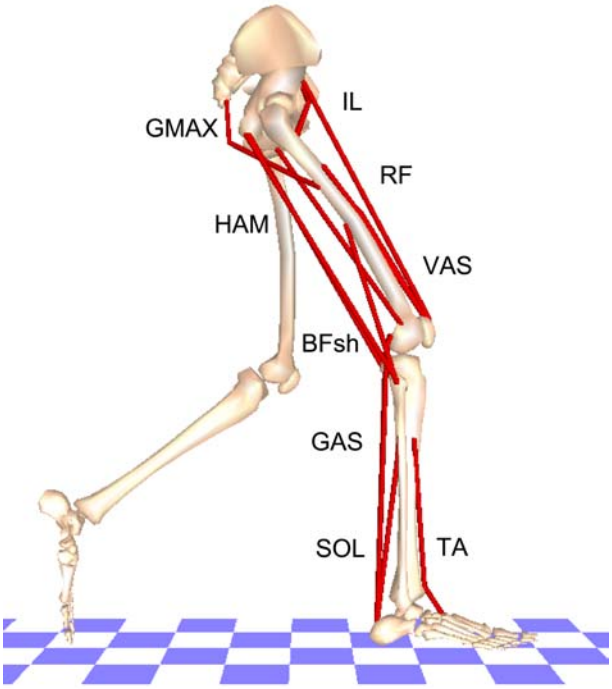

Fig. 1.1: The bipedal sagittal-plane musculoskeletal model

The model consisted of a HAT (head, arms and torso combined into one segment) and right and left legs (each leg containing a femur, tibia, patella and foot). The model was driven by nine muscle groups per leg, including GMAX (gluteus maximus, adductor magnus), IL (iliacus, psoas), HAM (biceps femoris long head, medial hamstrings), VAS (3-component vastus), RF (rectus femoris), BFsh (biceps femoris short head), TA (tibialis anterior), GAS (medial and lateral gastrocnemius) and SOL (soleus).

1.2 Dynamic optimization

Dynamic optimization was used to modify the muscle excitation patterns in order to generate a well-coordinated walking motion. Experimentally-collected EMG linear envelopes were used to define the muscle excitation patterns (see *Experimental Data Collection* below). For those muscles from which EMG data were not measured, a block excitation pattern was used (e.g., Neptune et al., 2001, 2004a, b). A simulated annealing optimization algorithm (Goffe et al., 1994) was used in the tracking optimization framework to modify the excitation onset, offset and magnitude until the difference between the experimental and simulated kinematic and GRF data was minimized (e.g., Neptune et al., 2001). Constraints were placed on the excitation timing in the optimization to closely replicate the EMG timing (i.e., EMG nominal values ± 10% gait cycle). Symmetry was assumed between the left and right legs. The specific tracking quantities included the trunk translations and rotation, all joint angles and the horizontal and vertical GRFs.

2 Muscle force and contractile state

To examine the stated hypothesis, the contractile state (i.e., muscle fiber length, fiber velocity), activation level and musculotendon force of each muscle were analyzed over the entire gait cycle. The fiber length and velocity were normalized to muscle's optimal fiber length (l_0) and maximum contraction velocity (estimated as $10l_0$; Zajac, 1989), respectively.

3. Experimental Data Collection

There were two phases of experimental data collection: 1) determination of each subject's walk-run PTS, and 2) collection of walking kinesiological data (i.e., body-segment kinematics, horizontal and vertical GRFs and EMG) at speeds of 60, 80, 100 and 120% PTS. Ten healthy subjects (5 males and 5 females: age 29.6 ± 6.1 years old, height 169.7 ± 10.9 cm, body mass 65.6 ± 10.7 kg) participated in the experiments. Informed consent, approved by the Cleveland Clinic Foundation and The University of Texas at Austin, was obtained from each subject before participating in the experiments. All data were collected at the Cleveland Clinic Foundation in Cleveland, OH.

3.1 Determining the preferred transition speed

After warming up and becoming familiar with the split-belt treadmill with embedded force plates (TecMachine[1], France), each subject started walking on the treadmill at 0.6 m/s. The subject was instructed to either walk or run with their preferred mode while the treadmill speed was systematically increased by 0.1 m/s every 30 seconds. This stepped protocol was continued to reach the point where the subject preferred running to walking during the entire 30-second interval, which was defined the subject's PTS for that trial. Three trials were conducted to obtain an average value of the PTS.

3.2 Data acquisition and processing

Kinematic, GRF and EMG data were collected during walking on the treadmill at the four speeds, which were randomly assigned, with the sampling frequencies of 120,

[1] URL: http://www.hef.fr/A20.HTML

480 and 1200 Hz, respectively. Each trial lasted approximately one minute while data were collected for a period of 15 seconds near the end of the one-minute duration. The kinematic data were collected with a Motion Analysis system (Motion Analysis Inc[1], Santa Rosa, CA). A modified Helen Hayes marker set (one-inch reflective markers) was used to define body segments. EMG data were collected from seven muscle groups of the right leg including the gluteus maximus, rectus femoris, vastus medialis, biceps femoris long head, medial gastrocnemius, tibialis anterior and soleus. After shaving and cleaning the skin with alcohol, disposable surface bi-polar EMG electrodes (Noraxon[2], Scottsdale, AZ) were attached to the muscle bellies using the guidelines provided by Perotto (1994). All data were digitally filtered using fourth-order zero-lag Butterworth filters. The GRF and kinematic data were low-pass filtered with the cutoff frequencies of 20 Hz (e.g., Antonsson and Mann, 1985) and 6 Hz (e.g., Winter, 1990), respectively. The EMG data were band-pass filtered (20-400 Hz), full-wave rectified and low-pass filtered (10 Hz) to produce linear envelopes (e.g., Gonzalez et al., 1996), and then normalized to the muscle's maximum value observed during walking at the highest speed. All data were time-normalized to the full gait cycle (i.e., from heel-strike to ipsilateral heel-strike) and averaged within, and then across subjects to obtain a group average.

[1] URL: http://www.motionanalysis.com/
[2] URL: http://www.noraxon.com/

RESULTS

The group average PTS was 1.96 ± 0.17 m/s. The tracking optimization algorithm was able to generate walking simulations of 60, 80, 100 and 120% PTS that closely matched the group average kinematics and GRFs (Fig. 1.2). The muscle excitation pattern and timing also compared well with the experimental EMG linear envelopes (Fig. 1.3). In general, the simulation muscle excitation magnitudes increased with walking speed in a similar fashion to the experimental data.

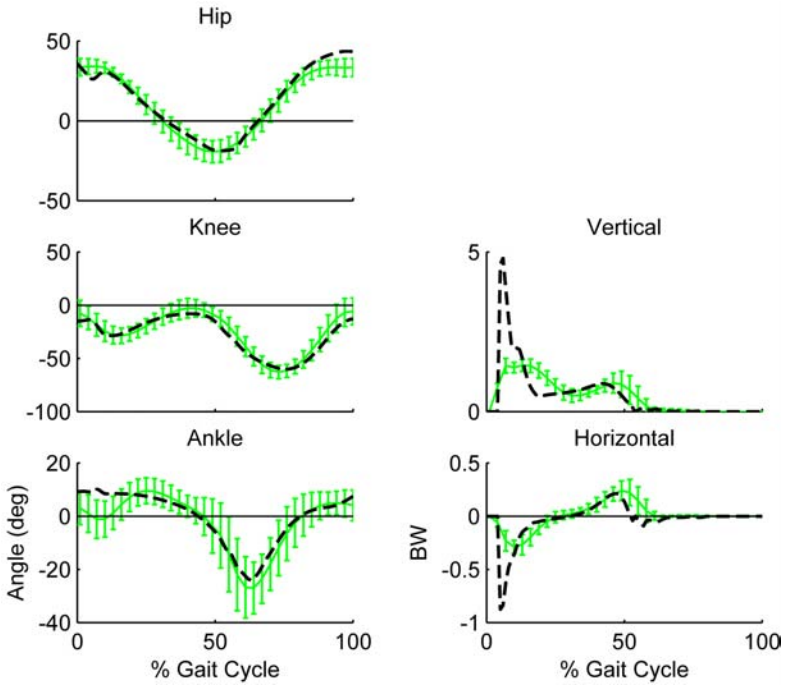

Fig. 1.2: Tracking results

Hip, knee and ankle joint angles and vertical and horizontal ground reaction forces in the walking simulation (dashed line) and experimental data (solid line, average ± 2 S.D.) at 120% PTS over the gait cycle (right heel-strike to right heel-strike). Similar tracking results were obtained for the 60, 80 and 100% PTS walking conditions. Positive angles indicate flexion, extension and dorsiflexion in the hip, knee and ankle joints, respectively.

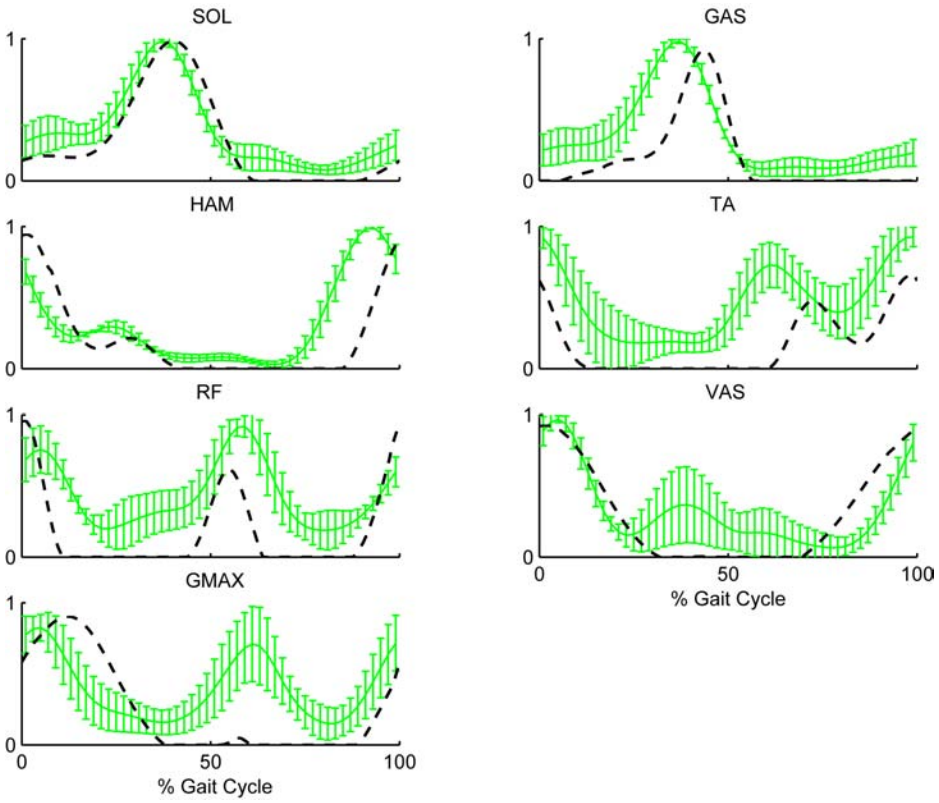

Fig. 1.3: Muscle excitation patterns

Simulation muscle excitation patterns (dashed line) and group average EMG linear envelopes (solid line, average ± S.D.) at 120% PTS over the gait cycle (right heel-strike to right heel-strike). The EMG data were normalized to the maximum value observed over the gait cycle for each muscle.

Contractile state and force production in the plantar flexors

The plantar flexors were active from mid- to late stance, with their magnitude systematically increasing with walking speed (Fig. 1.4C: 20 – 60% gait cycle). The SOL fiber length shortened from mid-stance to toe-off, with the rate of shortening systematically increasing with walking speed (Fig. 1.4B: 25 – 60% gait cycle). The peak shortening velocity of 0.3 was observed at toe-off (Fig. 1.4B: SOL, ~55% gait cycle).

The muscle fiber length shortened at the higher walking speeds and approached 0.5 l_o near toe-off (Fig. 1.4A: SOL, ~60% gait cycle). The length changes in GAS across walking speeds was not as large as SOL (Fig. 1.4A: GAS, ~25-55% gait cycle), although its shortening velocity increased more rapidly from mid- to late stance than SOL in all speeds (Fig. 1.4B: GAS, ~25-55% gait cycle). The combined effect of the contractile state (shortened fiber length and increased shortening velocity as speed increased) had a detrimental effect on the musculotendon force output. The maximum force across walking speeds occurred at 80% PTS in SOL (60% PTS in GAS) and then systematically decreased as walking speed increased despite an increase in muscle activity (Fig. 1.4C-D: SOL, GAS).

Contractile state and force production in other muscles

The contractile state of all the other muscle groups was more advantageous for producing muscle force. The force output continued to increase as muscle activity increased with walking speed. For example, both TA activation and corresponding force level increased with speed during the swing phase (Fig. 1.4C-D: TA, ~60 – 100% gait cycle). In this region, the TA fiber length approached its optimal length shortly after toe-off and remained above 0.75 l_0 throughout the remaining swing phase (Fig. 1.4A: TA, ~60-100% gait cycle) and its normalized shortening velocity never exceeded 0.23 (Fig. 1.4B: TA, ~70% gait cycle). The relationship between increased muscle activity and increased musculotendon force occurred in all muscle groups as walking speed increased, except for the plantar flexors (e.g., Fig. 1.4C-D: RF and HAM).

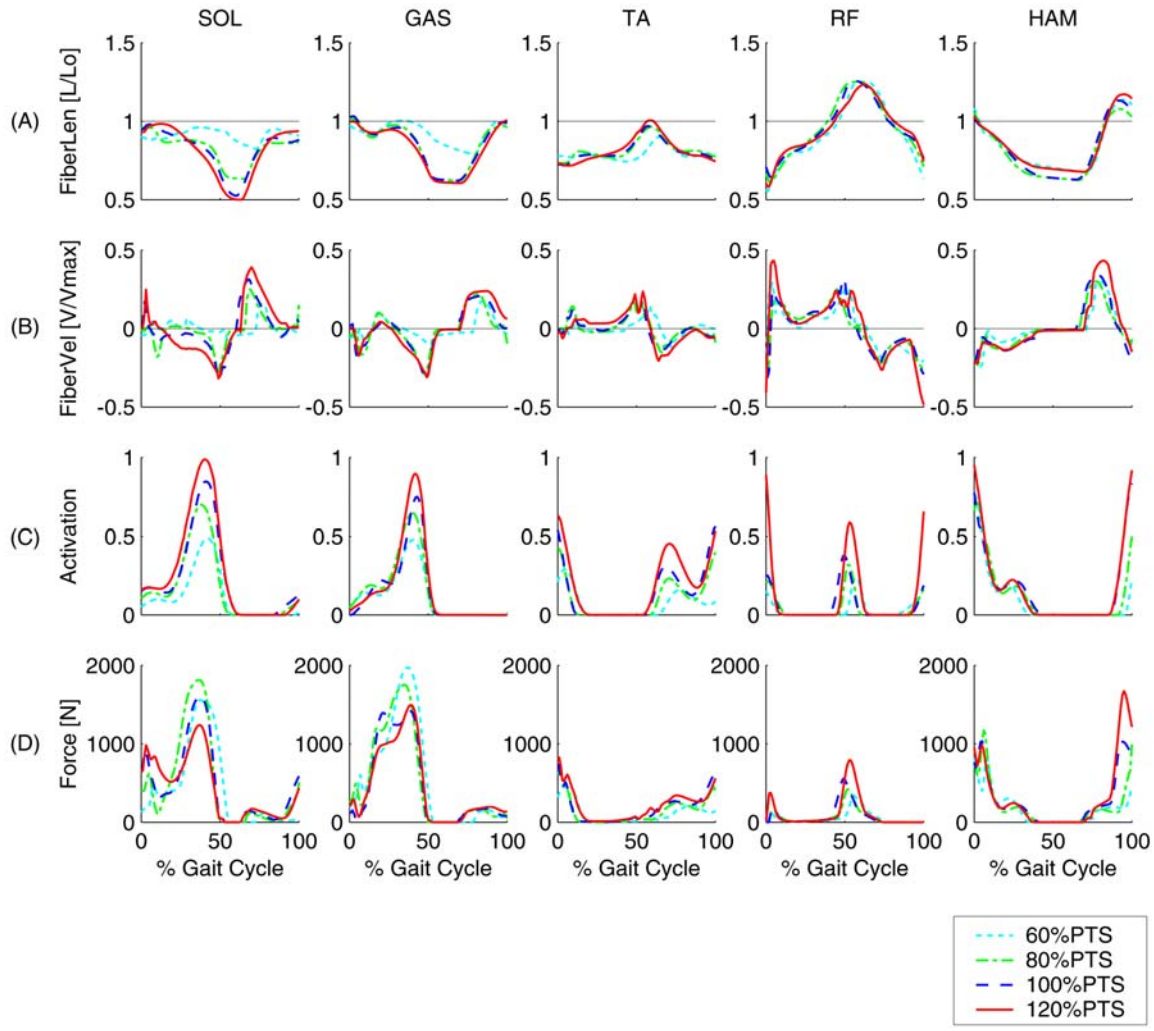

Fig. 1.4: Muscle contractile state, activation and force output

(A) normalized fiber length, (B) normalized fiber velocity, (C) activation level and (D) musculotendon force across increasing walking speeds in the soleus (SOL), gastrocnemius (GAS), tibialis anterior (TA), rectus femoris (RF) and hamstrings (HAM). A fiber length of 1 is equivalent to the optimal fiber length (l_0). Negative fiber velocity indicates fiber shortening.

DISCUSSION

The purpose of the present study was to investigate how contractile state, activation level and force production in the major lower-extremity muscle groups varied during walking at increasing speeds. These data were used to assess the hypothesis that muscle force production in the ankle plantar flexors is near its maximum capacity at the PTS, and therefore, serves as a determinant of the walk-run transition (Neptune and Sasaki, 2004). Because of the difficulty in identifying the contractile state of individual muscles *in vivo*, forward dynamic simulations of walking driven by individual Hill-type muscle actuators were used for the analyses.

The stated hypothesis was supported by the simulation data, which showed that the plantar flexors were the only muscle group to have a decrease in force output at the higher walking speeds despite a systematic increase in muscle activity (Fig. 1.4C-D: SOL, GAS ~20-60% gait cycle). The decreased force production at the higher speeds (80% PTS and greater) is attributed to the adverse contractile state of the muscles (fiber length and velocity) that becomes more detrimental at higher walking speeds (Fig. 1.4A-B: SOL, GAS). In both SOL and GAS, the fiber shortening velocity increases with walking speed because the rate of ankle plantar flexion increases (e.g., Neptune and Sasaki, 2004). The peak normalized velocity was near 0.3 at toe-off in both muscles when walking at 100% PTS. The simulation fiber velocities were consistent with velocity estimates from the force platform and kinematic measurements during normal walking (1.51 m/s) (Hof et al., 2002). Although the fiber velocity was not as unfavorable for producing muscle power as speculated by Neptune and Sasaki (2004), the continuous increase in shortening velocity associated with increasing speed caused a reduction in

force output in late stance at higher speeds. Previous modeling studies have shown that the ankle plantar flexors are critical in providing the necessary support, forward progression and swing initiation during normal walking (Neptune et al., 2001). Therefore, the reduced force output in these muscles near the PTS is detrimental to walking at higher speeds.

Although the increased fiber velocity impaired the plantar flexor force production, the decreased fiber length associated with increased walking speeds may have a more detrimental effect. The SOL and GAS fiber length shortened during ankle plantar flexion from mid- to late stance, with the magnitude of fiber shortening becoming more pronounced as speed increased (Fig. 1.4A: SOL and GAS). The normalized fiber length reached a peak value of 0.5 near toe-off at 100% PTS, which is far down the ascending portion of the force-length relationship (Fig. 1.5). These results differed with Hof et al. (2002), who estimated that the SOL fiber length at heel-strike was ~1.85 l_0, and then it shortened to ~ l_0 near toe-off. Some of the difference between these studies may be attributed to differences in the muscle force estimation. Hof et al. (2002) used inverse dynamics to obtain the SOL and GAS muscle forces, with an estimation error of ~ 20%. In addition, differences in musculoskeletal geometry and values used for the resting fiber and tendon slack lengths may also influence estimated fiber lengths. However, our results were consistent with Fukunaga et al. (2001), who measured *in vivo* GAS fiber length using ultrasonography during walking at 0.83 m/s. Their overall fiber length pattern was similar to our simulation results, although the fiber length was maintained ~0.85-0.9 l_0 throughout the stance phase. However, the difference in length change is most likely due to the difference in walking speed (0.83 m/s versus 1.2 m/s at 60% PTS), as our results show that the change in GAS fiber length becomes less at lower speeds (Fig. 1.4A: GAS).

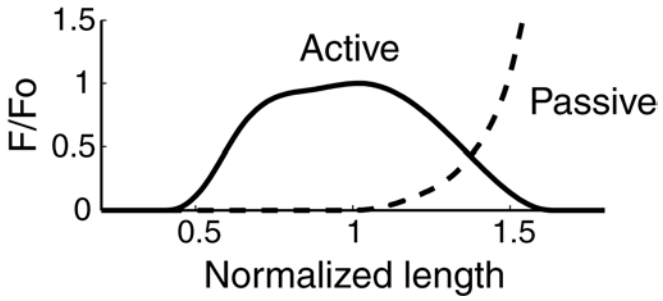

Fig. 1.5: Normalized muscle force-length relationship

The solid line represents the active fiber-force and the dashed line represents the passive force. The length and force were normalized to the optimal fiber length (l_0) and the maximum isometric force (F_0), respectively.

A potential limitation of our study (i.e., any modeling study) is that the contractile state of the muscles will be influenced by the specific parameters used in the model (e.g., optimal fiber length and pennation angle). The analyses of the plantar flexor pennation angles *in vivo* have shown that they can vary with isometric contraction intensity as well as the ankle and knee joint angles (Narici et al., 1996; Kawakami et al., 1998). For example, GAS pennation angle can vary from 17° (resting) to 35° (maximum isometric voluntary contraction) (Narici et al., 1996). The plantar flexor pennation angles in our model do not precisely reflect these changes. However, the muscle force is affected only by the cosine of pennation angle (e.g., Zajac, 1989), and therefore such variations may not have a large affect on the force-length relationship. Further study is needed to examine *in vivo* data for all muscle groups to quantify the influence of pennation angle on the contractile state of muscles during walking.

Neptune and Sasaki (2004) observed a decrease in experimentally measured GRFs as walking speed approached the PTS. They attributed the decrease to a reduction in plantar flexor force output since those muscles have been shown to be the primary

contributors to the GRFs during the propulsion phase in walking at self-selected speeds (Anderson and Pandy, 2003; Neptune et al., 2004a). Similar results were observed in the present simulation study. For example, the peak simulated horizontal GRF during the propulsion phase at 60, 80, 100 and 120% PTS were 10, 14, 22 and 21 % bodyweight, respectively. However, the plantar flexor force output began to decrease after 80% PTS (Fig. 1.4D: SOL, GAS), and therefore it is not clear why the peak horizontal GRF continued to increase up to 100% PTS. One explanation would be that other muscle groups increase their contribution to the horizontal GRF at higher walking speeds. To assess this possibility, we performed a GRF-decomposition based on our previous work (e.g., Neptune et al., 2001; Neptune et al., 2004a). We found the RF contribution to the horizontal GRF during the propulsion phase increased with walking speed and offset the decrease in the plantar flexor contribution. RF has been shown as an important contributor to forward progression in late stance along with the plantar flexors (Neptune et al., 2004a). In contrast to the plantar flexors, RF continued to increase its force output as activity increased with walking speed (Fig. 1.4C-D: RF).

The simulation results did not support the previous hypotheses that high levels of muscle activity in TA, RF and HAM during swing-phase serves as an important determinant of the gait transition (Hreljac, 1995a; Hreljac et al., 2001; Prilutsky and Gregor, 2001). The TA contractile state during the swing phase (~60-100% of gait cycle) was much more favorable than the contractile state of the plantar flexors. The normalized TA fiber length remained above ~0.75 (Fig. 1.4A: TA, 60-100% gait cycle) compared to the SOL fiber length that shortens to near 0.5 (Fig.4A: SOL, ~50% gait cycle). The TA has the advantage of a longer optimal fiber length (e.g., Wickiewicz et al., 1983), and therefore faster maximum contraction velocity (Zajac, 1989) than SOL, which provides a wider range of the contractile state for which the muscle can produce force.

Consequently, the TA is able to continue generating a high level of force as walking speed increases.

In addition to TA, Prilutsky and Gregor (2001) suggested that swing-phase RF and HAM activity are also important contributors to the gait transition. However, similar to TA, their contractile state was more favorable than the plantar flexors, as they continued to increase force production as muscle activity and walking speed increased (Fig. 1.4C-D: RF, HAM). Similarly, all other muscle groups increased their force production as muscle activity and walking speed increased.

In summary, the ankle plantar flexors were the only muscle group in which muscle force decreased despite an increase activity. This was due to intrinsic muscle properties at higher walking speeds. In addition, the muscle force-length relationship appeared to have a stronger influence on limiting the plantar flexor force output than the force-velocity relationship. Considering the important contributions of the plantar flexors to support, forward progression and swing initiation during mid- to late stance (e.g., Neptune et al., 2001; Zajac et al., 2003), these results support the hypothesis that impaired plantar flexor force production is an important determinant of the walk-run transition.

CHAPTER 2

Differences in muscle function during walking and running at the preferred transition speed

INTRODUCTION

Walking and running are the two most common forms of human gait. Understanding how individual muscles contribute to satisfying the different task requirements of walking and running may provide important insight into the neuromotor control strategies used during human locomotion. Many of the basic kinetics and kinematics of walking and running are similar (e.g., Nilsson et al., 1985; Nilsson and Thorstensson, 1989). However, one of the most noticeable differences is the existence of a flight phase in running rather than a double support phase in walking, which suggests the need for muscles to generate greater vertical acceleration of the body during the stance phase.

Recent modeling and simulation studies have identified how individual muscles satisfy the task requirements during normal walking. In the beginning of stance, body support (trunk upward acceleration) and forward progression (trunk forward acceleration) are provided by the uni-articular hip and knee extensors, while in late stance, the ankle plantar flexors are the primary contributors (Anderson and Pandy, 2003; Neptune et al. 2001, 2004a; Zajac et al., 2003). However, whether these same muscle groups are responsible for providing body support and forward progression in running remains unknown.

Interpretation of which muscles provide body support and forward progression in running has varied across previous inverse dynamics-based analyses. Some studies have suggested the knee extensors and ankle plantar flexors contribute to forward progression from mid- to late stance (Ounpuu, 1990; Novacheck, 1998), while other studies have concluded that the hip extensors are the primary contributors (Simonsen et al., 1985; Belli et al., 2002). Other EMG-based studies have suggested that the plantar flexors have little contribution to push-off in late stance since these muscles' peak activity occurs from the beginning to mid-stance and then decreases in late stance (e.g., Mann et al., 1986; Reber et al., 1993). Part of the discrepancy among studies could be related to the inability of inverse dynamics-based analyses to identify individual muscle contributions to the accelerations and energetics of individual body segments (Zajac et al., 2002). Identifying such contributions is crucial for assessing muscle function since the contributions can vary greatly even within the same muscle groups over a gait cycle (e.g., Neptune et al., 2001; Zajac et al., 2003).

By comparing individual muscle contributions between walking and running, differences and similarities of muscle function between the two different gait modes can be clarified. Analyzing how individual muscle contributions change at the same speed is particularly informative. Because many of the task requirements (e.g., the need for body support and forward progression) remain the same, such analysis would highlight the fundamental differences in muscle function during walking and running. For example, previous analysis of walking has shown that as walking speed increases, plantar flexor force production starts to decrease near the preferred walk-run gait transition speed (PTS) (Chapter 1) and that the force production increases after the transition to running (Neptune and Sasaki, 2004). However, how changes in the task mechanics (i.e., switching

from walking and running) influence the plantar flexors or any muscle's ability to contribute to body support and forward progression is not clearly understood.

Therefore, the overall goal of this study was to use forward dynamic simulations to identify quantitative and qualitative differences in muscle function during walking and running at the PTS. Forward dynamic simulations provide a powerful framework to precisely quantify how individual muscles contribute to achieving the task requirements in each gait mode. The specific objective was to access whether the contributions from the hip and knee extensors and plantar flexors to body support and forward progression remain invariant in walking and running, or whether individual muscles function differently in each gait mode, which would provide important insight into neuromotor principles governing human locomotion.

METHODS

1 Forward dynamics simulations

1.1 Musculoskeletal model

A 2D musculoskeletal model and forward dynamic simulations during both walking and running at the preferred gait transition speed (PTS) were generated to quantify individual muscle contributions to the body segment energetics including support and forward progression. The model and simulations were developed using SIMM (MusculoGraphics Inc.[1], Evanston, IL) and Dynamics Pipeline (MusculoGraphics Inc., Evanston, IL), respectively, and the equations of motion were generated using SD/FAST (PTC Inc.[2], Needham, MA). The musculoskeletal model included a trunk (head, arms, torso and pelvis) and right and left legs (femur, tibia, patella and foot), with nine degrees-of-freedom (hip, knee, ankle flexion/extension for both legs, and trunk horizontal and vertical translation and rotation). Two translational degrees-of-freedom of the tibia relative to the femur and three degrees-of-freedom of the patella relative to the tibia were prescribed as a function of the knee angle (Yamaguchi and Zajac, 1989; Delp, 1990). Fifteen Hill-type musculotendon actuators per leg were included to drive the model (Neptune at al., 2001, 2004a, b; Zajac et al., 2003). These muscles were combined into nine functional groups that received the same excitation patterns based on anatomical classification (Fig. 2.1: GMAX (gluteus maximus, adductor magnus), IL (iliacus, psoas), HAM (biceps femoris long head, medial hamstrings), VAS (3-component vastus), RF

[1] URL: http://www.musculographics.com/
[2] URL: http://www.ptc.com/

(rectus femoris), BFsh (biceps femoris short head), TA (tibialis anterior), GAS (medial and lateral gastrocnemius) and SOL (soleus)).

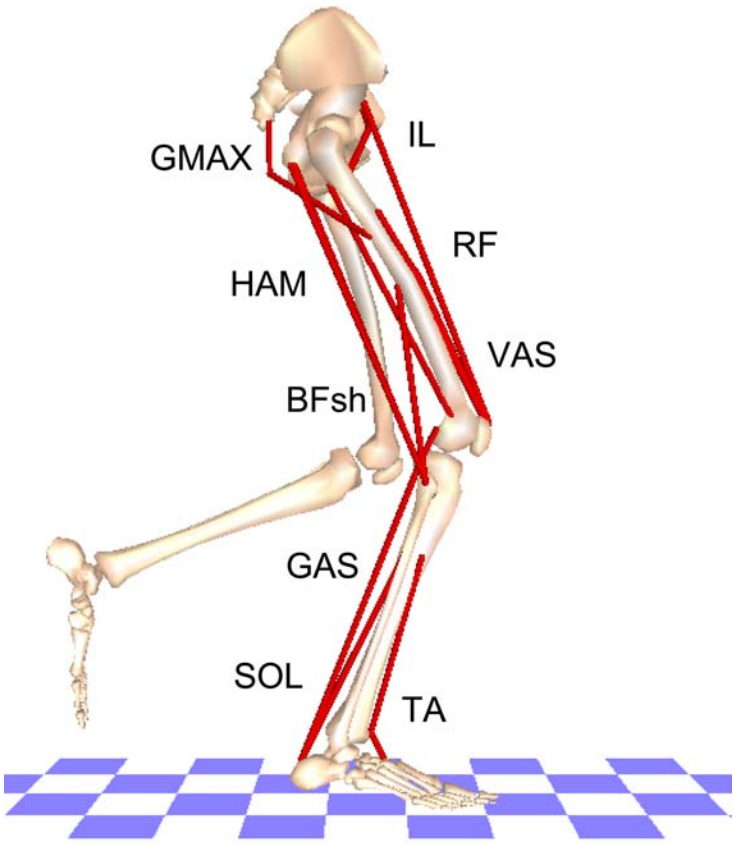

Fig. 2.1: The bipedal sagittal-plane musculoskeletal model

The 2D-musculoskeletal model consisting of the HAT (head, arms and torso) and right and left legs (femur, tibia, patella and foot). The nine muscle groups per leg were defined as GMAX (gluteus maximus, adductor magnus), IL (iliacus, psoas), HAM (biceps femoris long head, medial hamstrings), VAS (3-component vastus), RF (rectus femoris), BFsh (biceps femoris short head), TA (tibialis anterior), GAS (medial and lateral gastrocnemius) and SOL (soleus).

The excitation patterns of these muscle groups were based on EMG data (see *Experimental data collection* below). For the muscles from which EMG was not measured (i.e., IL and BFsh), a block excitation pattern was used (e.g., Neptune et al., 2001, 2004a, b). The muscle activation and deactivation dynamics were described by a first-order differential equation (Raasch et al., 1997) with activation and deactivation time constants of 5 and 10 ms, respectively. Passive torques were applied to each joint to represent ligaments and other connective tissues (Davy and Audu, 1987). The contact between the foot and ground was modeled using thirty visco-elastic elements attached to each foot segment (Neptune et al., 2000).

1.2 Dynamic optimization

Dynamic tracking optimization using a simulated annealing algorithm (Goffe et al., 1994) was employed to generate the simulations that emulate walking and running at the PTS by modifying the onset, duration and magnitude of the muscle excitation patterns. The objective function that was minimized in the optimization included the differences between the simulation and experimental kinematics (i.e., trunk rotation and translations, and all joint angles) and ground reaction forces (GRFs) over a gait cycle (see *Experimental data collection* below) (e.g., Neptune and Hull, 1998; Neptune et al., 2001; Zajac et al., 2003).

1.3 Muscle contributions to body support and forward progression

Individual muscle contributions to body support and forward progression over the gait cycle were quantified using muscle-included acceleration and segment power

analyses (Fregly and Zajac, 1996; Neptune et al., 2001, 2004a; Zajac et al., 2003). The system equations of motion are expressed as:

$$\ddot{q} = M^{-1}(q)D^{m} \cdot F(q,\dot{q},a) + M^{-1}(q)G(q) + M^{-1}(q)V(q,\dot{q}) + M^{-1}(q)T(q,\dot{q}) \qquad (2.1)$$

where q, $\dot{q}$, and $\ddot{q}$ are the generalized coordinates, first and second time derivatives, respectively (9 by 1), a is muscle activation level (30 by 1), $M(q)$ is the system mass matrix (9 by 9), D^{m} is the muscle moment-arm matrix (9 by 30), $F(q,\dot{q},a)$ is the musculotendon actuator force vector (30 by 1), $G(q)$ is the gravitational force vector (9 by 1), $V(q,\dot{q})$ is the Coriolis and centripetal force vector (9 by 1), and $T(q,\dot{q})$ is the ground reaction force vector (9 by 1). These accelerations on the right hand side may be re-written as the contributions from each component as:

$$\ddot{q} = \ddot{q}_{\text{muscle}} + \ddot{q}_{\text{gravity}} + \ddot{q}_{\text{velocity}} + \ddot{q}_{\text{GRF}} \qquad (2.2)$$

Therefore the muscle-induced accelerations can be obtained by applying only the muscle force of interest and its corresponding GRFs to the system (Neptune et al., 2001). A muscle's contribution to body support and forward progression was defined as its contribution to the trunk's vertical and horizontal acceleration, respectively.

Segment power analysis is a state-space power analysis (Fregly and Zajac, 1996). By definition (Kane and Levinson, 1985), system mechanical power is expressed as:

$$P = \frac{d}{dt}(KE + PE) = [M(q)\ddot{q} - V(q,\dot{q}) - G(q)]^{T}\dot{q} \qquad (2.3)$$

where *KE* and *PE* are the system kinetic energy and potential energy, respectively, and the superscript *T* represents the transpose of the matrix. Combining equations (2.1) and (2.3), segment power P_i is expressed as:

$$\begin{aligned} P_i &= [M_i(q)\ddot{q} - V_i(q,\dot{q}) - G_i(q)]^T \dot{q} \\ &= [M_i(q)\ddot{q}_{muscle}]^T \dot{q} \\ &+ [M_i(q)\ddot{q}_{gravity} - G_i(q)]^T \dot{q} + [M_i(q)\ddot{q}_{velocity} - V_i(q,\dot{q})]^T \dot{q} + [M_i(q)\ddot{q}_{GRF}]^T \dot{q} \end{aligned} \tag{2.4}$$

where the subscript *i* on the right hand side indicates that only the component associated with segment *i* appears in the matrices or vectors (Fregly and Zajac, 1996). Therefore, the segment power generated, absorbed or transferred by a muscle is determined by current states (positions and velocities) and the muscle-induced accelerations.

The muscle-induced accelerations were time-normalized to the stance phase in order to directly compare walking and running, and segment power was time-normalized to a full gait cycle (i.e., from right foot-strike to right foot-strike).

2 Experimental data collection

Experimental data were collected to obtain the PTS from walking to running, and to acquire kinematic, GRF and EMG data that were used in the dynamic optimization to generate the simulations. Ten healthy subjects (5 males and 5 females: age 29.6 ± 6.1 years old, height 169.7 ± 10.9 cm, body mass 65.6 ± 10.7 kg) participated in the experiments. Informed consent approved by the Cleveland Clinic Foundation and The University of Texas at Austin was obtained from each subject before participating in the experiments. All data were collected at the Cleveland Clinic Foundation in Cleveland, OH.

2.1 Determining the preferred transition speed

Each subject's PTS from walking to running was determined on a split-belt treadmill with embedded force plates (TecMachine[1], France). After warming up and becoming familiar with the treadmill, each subject was instructed to walk starting at 0.6 m/s. Every 30 seconds, the treadmill speed was increased by 0.1 m/s. This increment was continued to reach the speed at which the subject switched from walking to running and preferred to run for the entire 30-second interval, and that speed was defined as the subject's PTS for the trial. Three trials were conducted to determine the average PTS.

2.2 Data acquisition and processing

The kinematic, GRF and EMG data were measured for 15 seconds near the end of the one-minute trial while walking or running on the treadmill at the PTS with sampling frequencies of 120, 480 and 1200 Hz, respectively. The kinematic data were captured using Motion Analysis system (Motion Analysis[2], Santa Rosa, CA) with a modified Helen Hayes marker set using one-inch diameter reflective markers. The EMG was collected from the right leg muscles using disposable surface bi-polar EMG electrodes (Noraxon[3], Scottsdale, AZ) attached to the following muscle bellies using the guidelines provided by Perotto (1994): the gluteus maximus, rectus femoris, vastus medialis, biceps femoris long head, medial gastrocnemius, soleus and tibialis anterior. All data were digitally filtered using fourth-order zero-lag Butterworth filters. The cut-off frequencies for the kinematic and GRF data were 6 and 20 Hz, respectively (e.g., Winter, 1990;

[1] URL: http://www.hef.fr/A20.HTML
[2] URL: http://www.motionanalysis.com/
[3] URL: http://www.noraxon.com/

Antonsson and Mann, 1985). EMG linear envelopes were obtained through band-pass filtering (20-400 Hz), full rectification and low-pass filtering (10 Hz) (e.g., Gonzalez et al., 1996), and normalizing the amplitude to its maximum value observed during running for each muscle. The data were time-normalized to a full gait cycle, averaged within each subject, and then across all subjects to obtain a group average.

RESULTS

Walking/running simulation results

The generated simulations of walking and running at the PTS (1.96 ± 0.17 m/s: group average and S.D.) matched the group-averaged kinematics and ground reaction forces, with most tracking variables within ± 2 S.D. (Fig. 2.2).

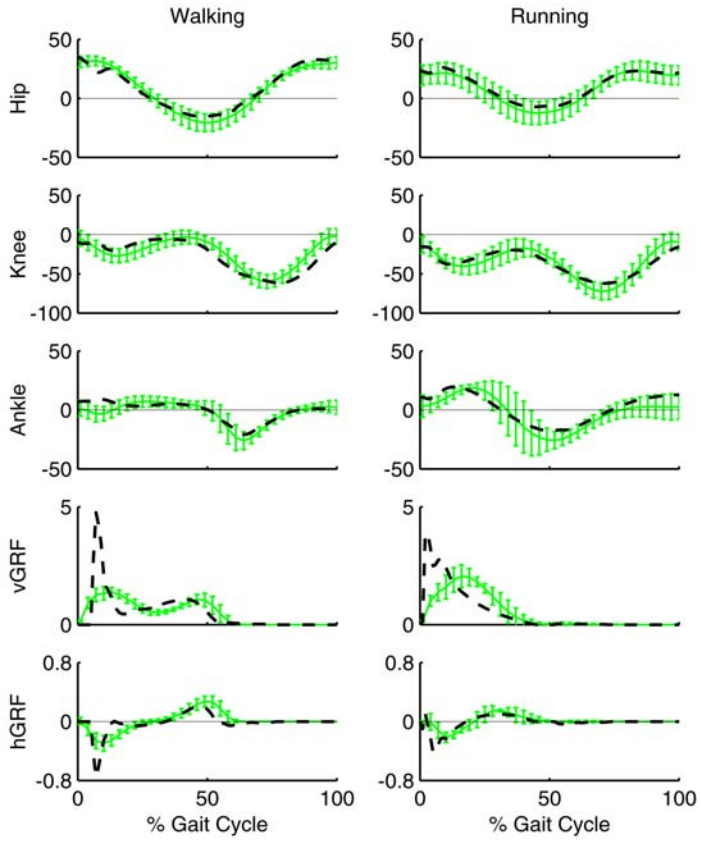

Fig. 2.2: Tracking results

Hip, knee and ankle joint angles (units: degrees) and vertical (vGRF) and horizontal (hGRF) ground reaction forces (units: normalized to body weight) in walking and running simulations (dashed line) and experimental data (solid line, average ± 2 S.D.) at the preferred transition speed. Positive angles indicate flexion, extension and dorsiflexion in the hip, knee and ankle joints, respectively.

In the running simulation, the angle between the foot and ground was near zero at foot-strike (i.e., the simulation represented a mid-foot strike), which was consistent with the average subject pattern. The corresponding muscle excitation patterns also compared well with human subject EMG linear envelopes (Fig. 2.3).

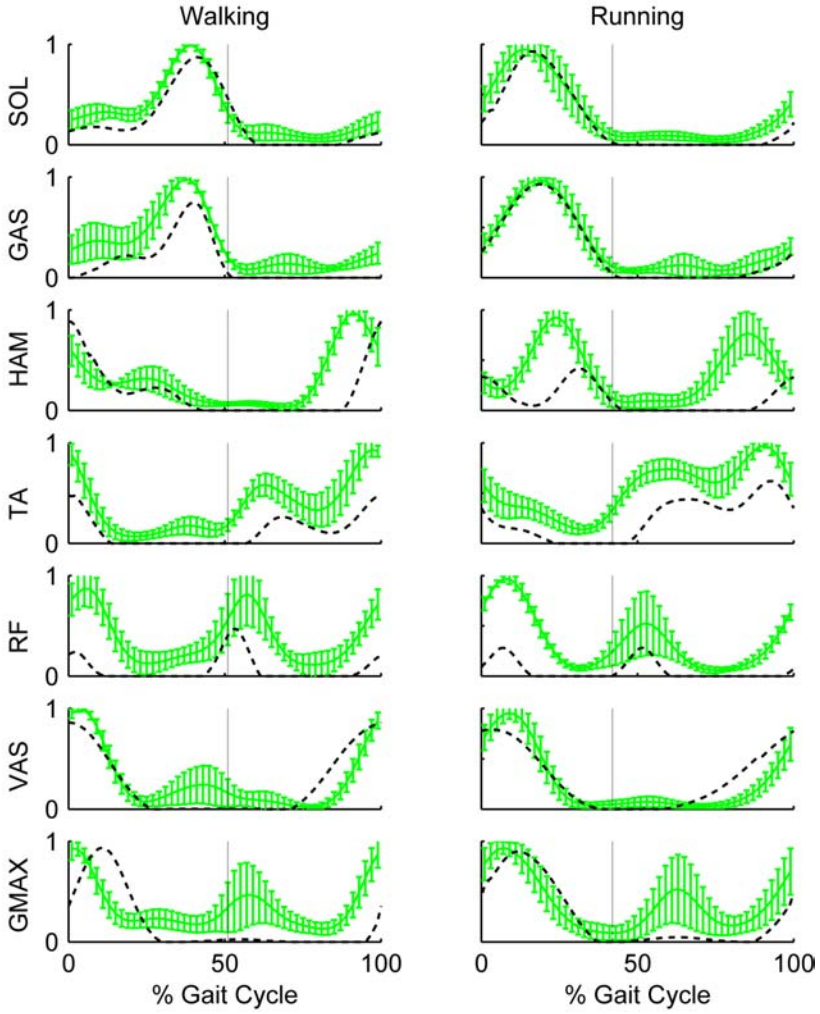

Fig. 2.3: Muscle excitation patterns

Muscle excitation patterns for the walking and running simulations (dashed line) and group average EMG linear envelopes (solid line, average ± S.D.) at the preferred transition speed. The EMG data were normalized to the maximum value observed over the gait cycle for each muscle. The vertical lines indicate toe-off.

Muscle segmental power distribution

Distinctive differences between walking and running were observed in the distribution of mechanical power generated by SOL. In walking, SOL absorbed ipsilateral leg power and transferred much of that power to the trunk from mid- to late stance, then in late stance, simultaneously generated power directly to the trunk (Fig. 2.4a: SOL, Walking ~ 25-50% gait cycle). In running, SOL initially absorbed power from both the leg and trunk in the beginning of stance (Fig. 2.4a: Running, 0–15% gait cycle) and then generated power to both the leg and trunk during mid-stance (Fig. 2.4a: Running, ~15-30% gait cycle). In contrast, GAS power distribution pattern was consistent between walking and running. The muscle delivered power to the leg in both walking (Fig. 2.4a: GAS, Walking, ~30-50% gait cycle) and running (Fig. 2.4a: GAS, Running, ~20-40% gait cycle). Consequently, GAS was in opposition to the SOL in leg-power distribution during walking, while it co-functioned with SOL to distribute power to the leg during running.

VAS was the largest power-producing muscle and exhibited similar power distribution patterns in both walking and running. VAS initially absorbed power from both the leg and trunk in the beginning of stance (Fig. 2.4b: VAS, Walking, 0-5% gait cycle, Running, 0-15% gait cycle), and then generated power to the trunk while simultaneously absorbing power from the leg and delivering it to the trunk (Fig. 2.4b: VAS, Walking ~5-20% gait cycle, Running ~15-35% gait cycle). The magnitude of VAS power was much greater in running and extended into late stance (Fig. 2.3: VAS, Running), as opposed to walking where VAS activity ended in the beginning of stance (Fig. 2.3: VAS, Walking). Similarly, GMAX delivered power to the trunk while absorbing leg power in both walking and running (Fig. 2.4c: GMAX, Walking ~10-25% gait cycle, Running ~10-40% gait cycle).

Eccentric RF activity acted to transfer power from the leg to the trunk in both walking and running, although both the magnitude and timing were different. In walking, RF functioned primarily in late stance, while in running much lower power was distributed near mid-stance (Fig. 2.4c: RF, Walking, ~40-60% gait cycle, Running ~ 10–35 % gait cycle).

The magnitude of HAM power distribution was larger in walking in the beginning of stance. The muscles absorbed power from the trunk and delivered power to the leg (Fig. 2.4b: HAM, 0-10% gait cycle), then continued to generate power to the leg until mid-stance (Fig. 2.4b: HAM, Walking, ~10-30% gait cycle). From mid- to late swing, the muscles' eccentric action absorbed the leg power in both walking and running (Fig. 2.4b: HAM, ~75-95% gait cycle), then just before foot-strike, HAM concentric action delivered power to the leg only in walking (Fig. 2.4b: HAM, Walking, ~95-100% gait cycle). A distinctive difference between walking and running during stance was that HAM activity was increased in late stance in running (Fig. 2.3: HAM, Running, ~20-40% gait cycle) and power was delivered to the leg during this period (Fig. 2.4b: HAM, Running). BFsh functioned antagonistically with VAS in both walking and running. It delivered power to the trunk in the beginning of stance (Fig. 2.4b: BFsh, Walking, 0-5% gait cycle, Running, 0-15% gait cycle), and then absorbed power from the trunk and delivered it to the leg (Fig. 2.4b: BFsh Walking, ~5-20% gait cycle, Running ~15-35% gait cycle).

TA delivered power to the trunk in both walking and running in the beginning of stance (Fig. 2.4a: TA, Walking, 0-10% gait cycle, Running, 0-15% gait cycle). During mid-swing, the muscle delivered power to the leg in both walking and running (Fig. 2.4a: TA, Walking, ~60-75% gait cycle, Running, ~55-80% gait cycle). IL distributed power from the trunk to the leg in addition to the power that it generated to the leg from late

stance to mid-swing in walking (Fig. 2.4c: IL, Walking, ~40-75% gait cycle) and from the beginning to late swing in running (Fig. 2.4c: IL, Running, ~50-90% gait cycle). The magnitude of IL power was slightly larger in walking.

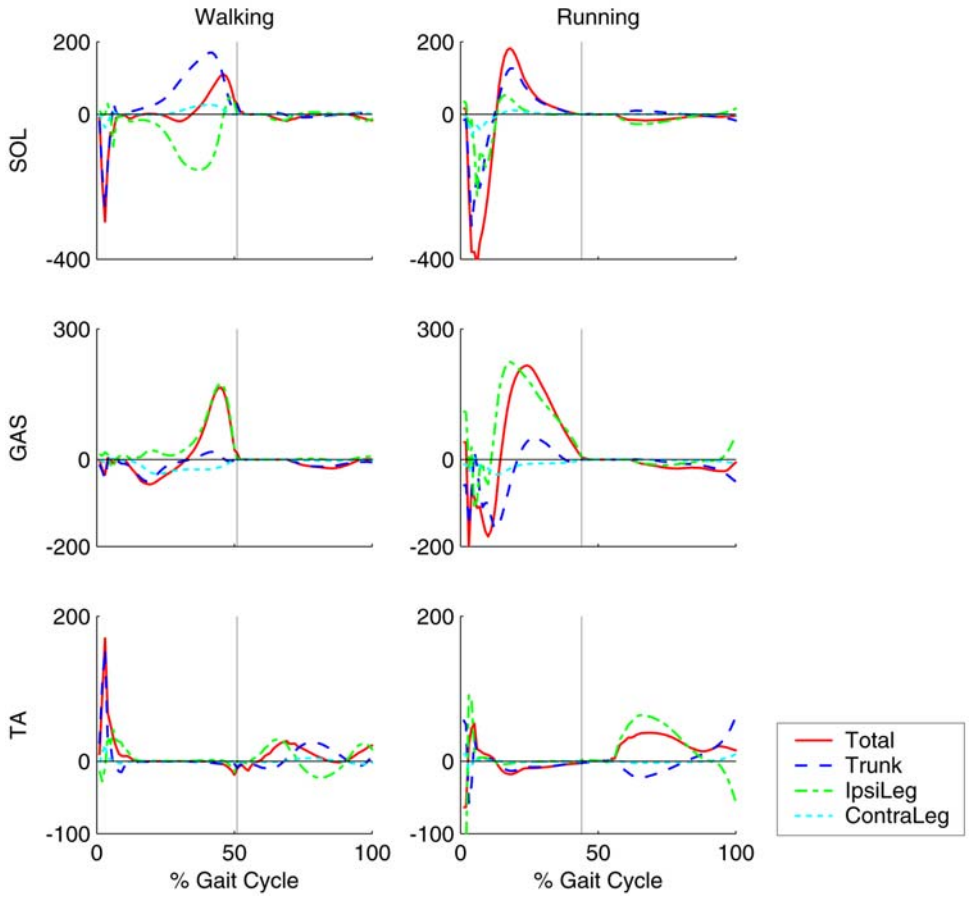

Fig. 2.4a: Segment power by SOL, GAS and TA

Distribution of muscle mechanical power (units: watts) to the trunk (Trunk), ipsilateral leg (IpsiLeg) and contralateral leg (ContraLeg) during walking and running at the preferred transition speed over the gait cycle (right foot-strike to right foot-strike). The vertical lines indicated toe-off.

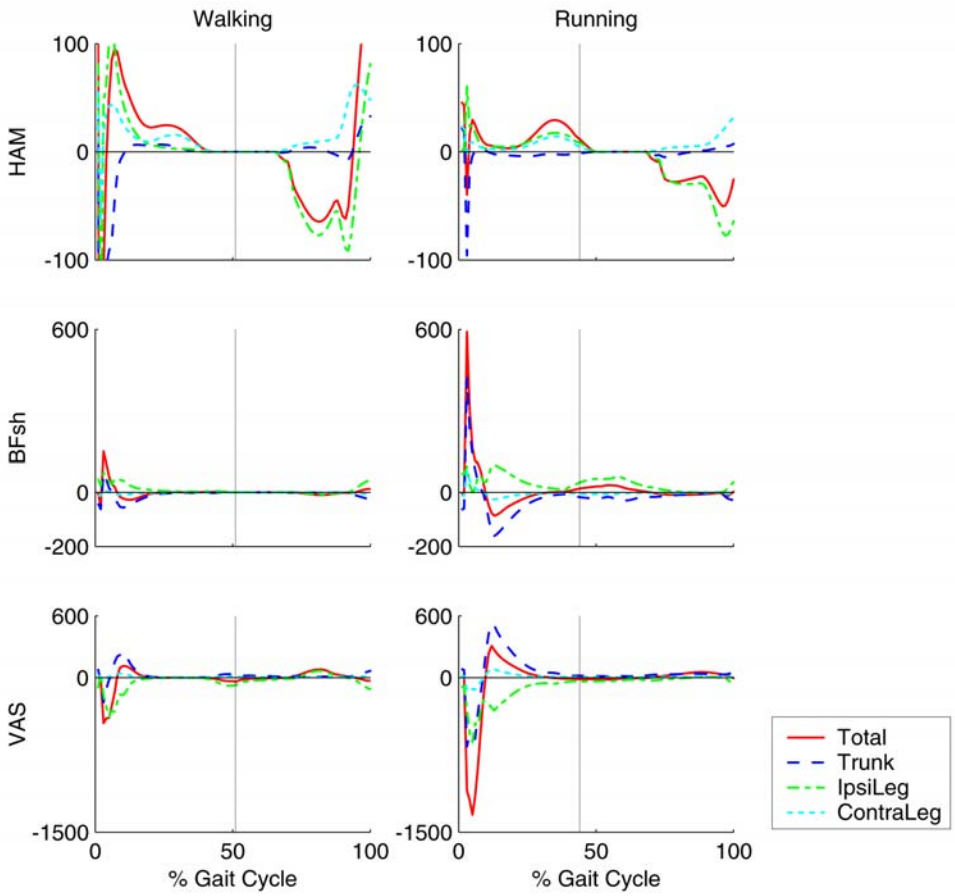

Fig. 2.4b: Segment power by HAM, BFsh and VAS

Distribution of muscle mechanical power (units: watts) to the trunk (Trunk), ipsilateral leg (IpsiLeg) and contralateral leg (ContraLeg) during walking and running at the preferred transition speed over the gait cycle (right foot-strike to right foot-strike). The vertical lines indicated toe-off.

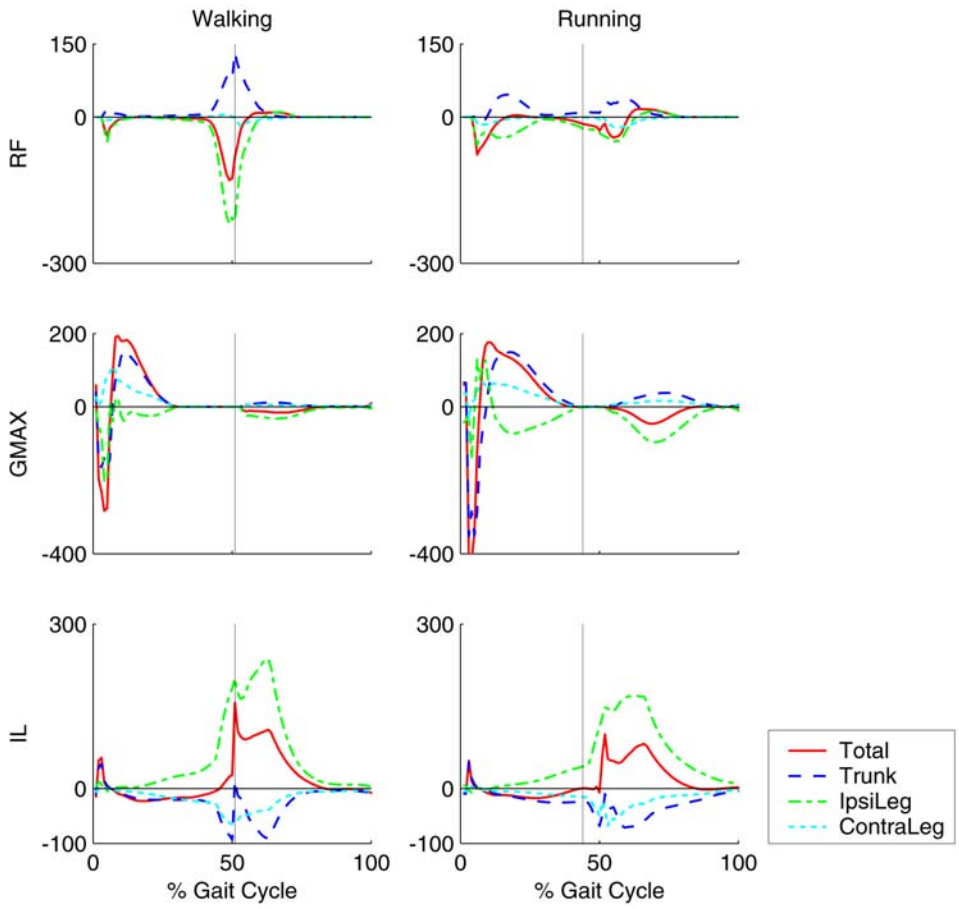

Fig. 2.4c: Segment power by RF, GMAX and IL

Distribution of muscle mechanical power (units: watts) to the trunk (Trunk), ipsilateral leg (IpsiLeg) and contralateral leg (ContraLeg) during walking and running at the preferred transition speed over the gait cycle (right foot-strike to right foot-strike). The vertical lines indicated toe-off.

Forward progression (horizontal trunk acceleration) during stance

In walking, SOL was the primary contributor to forward progression during late stance (Fig. 2.5: SOL, Horizontal, dashed line ~50-100% stance). GAS acted to decelerate the trunk near mid-stance (Fig. 2.5: GAS, Horizontal, dashed line, ~20-40% stance), and then provided some forward progression, co-functioning with SOL (Fig. 2.5: GAS, Horizontal, dashed line, ~60-100% stance). In running both SOL and GAS decelerated the trunk more strongly from the beginning to mid-stance (Fig. 2.5: SOL, Horizontal, solid line, 0-40% stance, GAS, Horizontal, solid line, ~10-60% stance) and provided negligible forward progression in late stance (Fig. 2.5: SOL, Horizontal, solid line, ~50-100% stance, GAS, Horizontal, solid line, ~70-100% stance).

In walking, VAS and GMAX decelerated the trunk in the beginning of stance (Fig. 2.5: VAS, GMAX, Horizontal, dashed line, 0-20% stance), and then accelerated the trunk with prolonged GMAX contribution (Fig. 2.5: VAS, Horizontal, dashed line, ~20-40% stance, GMAX, Horizontal, dashed line, ~20-60% stance). In running, these muscles showed lesser deceleration in the beginning of stance (Fig. 2.5: VAS, GMAX, Horizontal, solid line, 0-10% stance) and larger forward acceleration that extended into late stance (Fig. 2.5: VAS, Horizontal, solid line, ~10-80% stance, GMAX, Horizontal, solid line, ~20-80% stance) as a result of their prolonged activity into late stance (Fig. 2.3).

BFsh provided small contributions to forward progression in the beginning of stance in both walking and running (Fig. 2.5: BFsh, Horizontal, ~5-15% stance), then had little effect on the trunk in walking while acting to decelerate the trunk in running during mid-stance (Fig. 2.5: BFsh, Horizontal, ~20–75% stance). HAM provided negligible forward progression in both walking and running with a brief region of deceleration just after foot-ground contact in walking (Fig. 2.5: HAM, Horizontal, dashed line, 0-5%

stance). RF provided forward progression during late stance in walking (Fig. 2.5: RF, Horizontal, dashed line, ~80-100% stance), which was not observed in running. Instead, the muscle provided small forward progression in mid-stance (Fig. 2.5: RF, Horizontal, solid line, ~20-60% stance). TA had small contribution in the beginning of the stance in walking (Fig. 2.5: TA, Horizontal, dashed line, 0-10% stance), but the contribution was negligible in running. IL had negligible contributions to forward progression in both walking and running.

Body support (vertical trunk acceleration) during stance

In walking, the primary contributors to body support were VAS and GMAX in the beginning of stance (Fig. 2.5: VAS, GMAX, Vertical, dashed line, 0–30 % stance), and SOL and GAS from mid- to late stance (Fig. 2.5: SOL, Vertical, dashed line, ~50-100% stance, GAS, Vertical, dashed line, ~ 25–100% stance). In running, body support was provided by these same muscles, with VAS being the primary contributor. The SOL contribution to support occurred earlier in the stance phase as a result of its earlier excitation timing (Fig. 2.3: SOL), which was slightly delayed compared to the VAS and GMAX contributions (Fig. 2.5: VAS, GMAX, Vertical, solid line, 0-30% stance). The GAS contribution was delayed further into mid- to late stance (Fig. 2.5: GAS, Vertical, solid line, ~25-90% stance).

BFsh offset some of the body support provided by SOL, GAS, VAS and GMAX by acting to decelerate the trunk downward in both walking and running (Fig. 2.5: BFsh, Vertical, dashed line, ~5-40% stance, solid line, ~5-60% stance). HAM body support in the beginning of stance was much larger in walking than in running (Fig. 2.5: HAM, Vertical, dashed line, 0-5% stance). In walking, RF provided a small amount of body support in the beginning of stance and in late stance (Fig. 2.5: RF, Vertical, dashed line,

~5-20% and ~80-100% stance), while in running the contribution occurred from the beginning to mid-stance (Fig. 2.5: RF, Vertical, solid line, ~10-60% stance). Both TA and IL contributions to support were negligible.

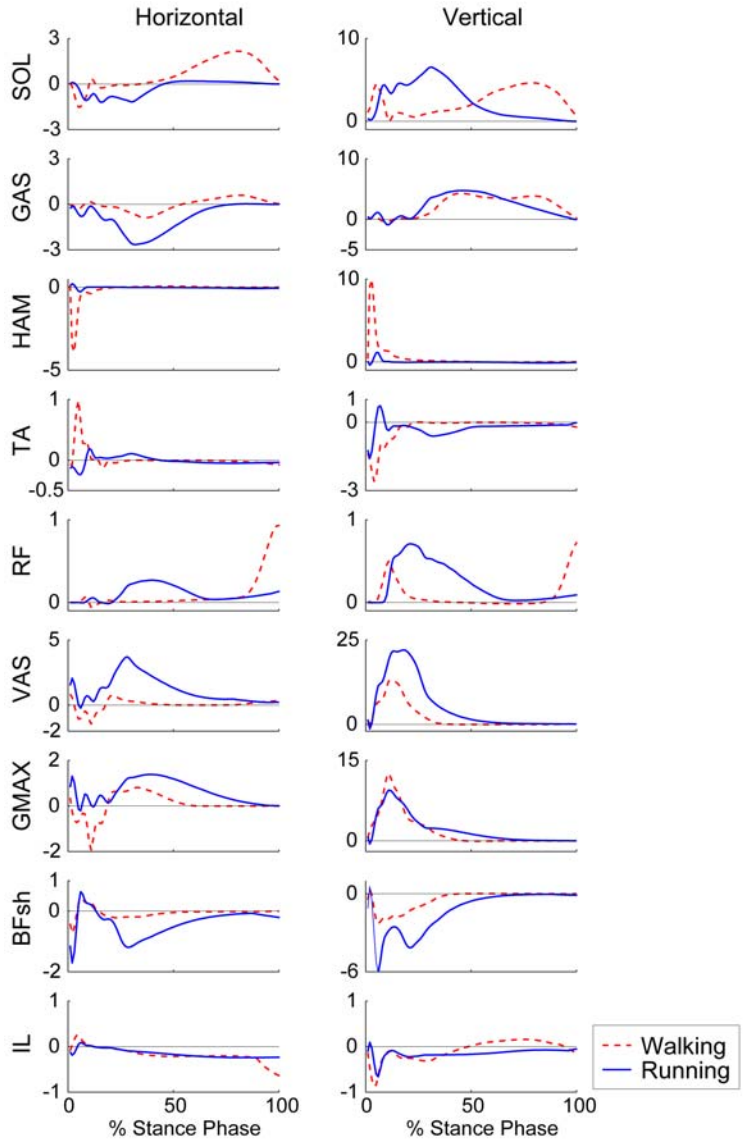

Fig. 2.5: Muscle-induced accelerations

Trunk horizontal and vertical muscle-induced accelerations (units: m/s^2) during stance in walking (dashed line) and running (solid line). The stance phase is defined from foot-strike to toe-off of the ipsilateral leg.

DISCUSSION

The overall goal of this study was to use forward dynamic simulations of walking and running at the preferred transition speed (PTS) in order to identify quantitative and qualitative differences in muscle contributions to body support and forward progression. Such an analysis will provide insight into neuromotor control strategies used in the two different gait modes. The simulations successfully emulated the salient features of kinesiological data collected from a group of healthy subjects walking and running at the PTS. The muscle-induced accelerations and segment power analysis were used to quantify the muscle contributions to the trunk accelerations and the mechanical energetics of the body segments.

The limitations of the walking and running simulations used in this study will be discussed first. Previous studies using a similar sagittal-plane musculoskeletal model have presented in detail the limitations of such models in the interpretation of muscle function (Neptune et al., 2001, 2004a ,b; Zajac et al., 2003). Unique to the present study was the difficulty we experienced in reproducing the vertical ground reaction force (GRF), especially in running (Fig. 2.2: Running, vGRF). We decomposed the GRFs into individual force contributions (e.g., Neptune et al., 2004a) and found that the impact peak (Fig. 2.2: Running, vGRF, 0-5% gait cycle) was composed primarily of non-muscular forces (i.e., gravity and velocity-dependent force). This initial spike was due to the use of a purely rigid-body model and may be improved by adding additional degrees-of-freedom and wobbling masses that would act as viscous dampers at impact (e.g., Schache et al., 1999; Liu and Nigg, 2000). The vertical GRF from the beginning to mid-stance was attributed to the force development in VAS and GMAX, and the difference between

the simulation and experimental GRF in this region (Fig. 2.2: Running, vGRF ~5-30% gait cycle) was primarily due to the constraints on the VAS excitation pattern in the optimization process using only three parameters (i.e., onset, offset and amplitude) to vary its pattern. The VAS excitation based on group-averaged EMG linear envelope tended to compromise the accuracy of either the knee joint angle in late swing or the vertical GRF from the beginning to mid-stance. However, we performed sensitivity analyses and found that in other running simulations with improved vertical GRF tracking (at the cost of increased deviation in joint angles, or using different VAS excitations such as a block pattern), the overall interpretation of individual muscle contributions to body support and forward progression were not altered (see Appendix 3).

Another possible limitation is exclusion of the upper-extremities in the simulation. The primary role of arm-movement during running is to provide the angular momentum along the long axis of the body that counteracts the momentum in the lower body for stabilization (Hinrichs, 1990). In addition, the upper-extremities provide impulses in the vertical direction that possibly contributes to body support. However, such contribution appears low (~5% of the total impulse) during stance and tends to be smaller at slower running speeds (Hinriches, 1990).

Body support was provided by the same muscle groups in both walking and running. Although SOL and GAS excitation in running occurred earlier in stance compared to walking (Fig. 2.3: SOL, GAS, also Mann et al., 1986; Reber et al., 1993), these muscles remain as the primary contributors with VAS and GMAX (Fig. 2.6: Running, Vertical). In contrast to body support, there were fundamental differences in muscle contributions to forward progression. SOL, and to a lesser degree GAS, contributed much during walking in late stance, but contributed little to forward progression in running. Instead, VAS was the primary contributor in running over the

stance phase, with peak contribution occurring at ~25% of stance (Fig. 2.5: VAS, Horizontal, solid line). GMAX also showed a substantial contribution near mid-stance (Fig. 2.5: GMAX, Horizontal, solid line, ~40% stance). The dominant VAS and GMAX contributions to forward progression in running are in agreement with previous studies suggesting that the hip and knee extensor muscles are the primary contributors (e.g., Simonsen et al., 1985; Novacheck, 1998; Simpson and Bates, 1990; Belli et al., 2002).

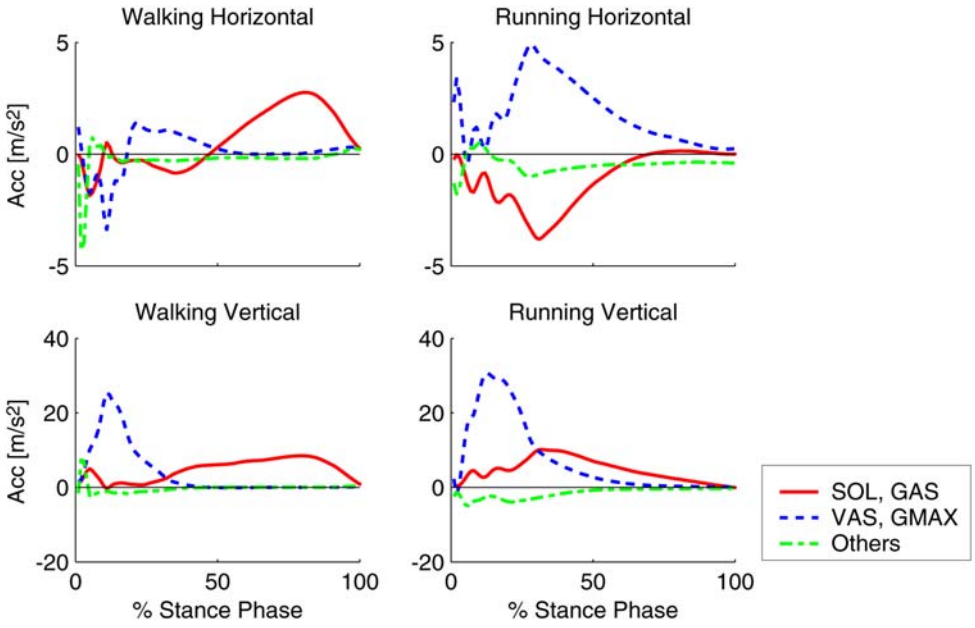

Fig. 2.6: Muscle-induced accelerations (combined)

Combined muscle-induced trunk horizontal and vertical acceleration during stance in walking and running at the preferred transition speed by SOL and GAS (SOL, GAS), VAS and GMAX (VAS, GMAX) and all other muscles combined (Others).

The decreased plantar flexor contribution to forward progression in running (especially SOL, Fig. 2.5: SOL, Horizontal, solid line) was surprising considering the increase in power production by SOL and GAS during running compared to walking

(Fig. 2.4a: SOL, GAS, Total, Walking and Running). The increase in power is attributed to an increase in force output (Neptune and Sasaki, 2004). However, because of the different task mechanics during running, the increased force production resulted in an increase in body support, rather than forward progression (Fig. 2.6: SOL, GAS, Running, Horizontal, Running, Vertical). The increase in body support by SOL and GAS from the beginning to mid-stance, combined with the support from VAS and GMAX that occurred slightly earlier in stance, resulted in the subsequent flight phase that was not observed during walking.

The most noticeable differences in individual muscle function between walking and running were observed in SOL. In addition to its decreased contribution to forward progression in running, the distribution of body segment power exhibited different patterns between walking and running. In walking, concentric SOL action in late stance absorbed leg power and delivered that power to the trunk (Fig. 2.4a: SOL Walking ~30-50% gait cycle), while in running SOL initially absorbed power from both the leg and trunk, and subsequently returned much of that power to the same segments (Fig. 2.4a: SOL Running, 0-30% gait cycle). The power delivered to the trunk was primarily in the horizontal direction in walking to produce forward progression, while the power was in the vertical direction in running to provide support near mid-stance (Fig. 2.7: Walking ~50-100% stance, Running ~20-60% stance).

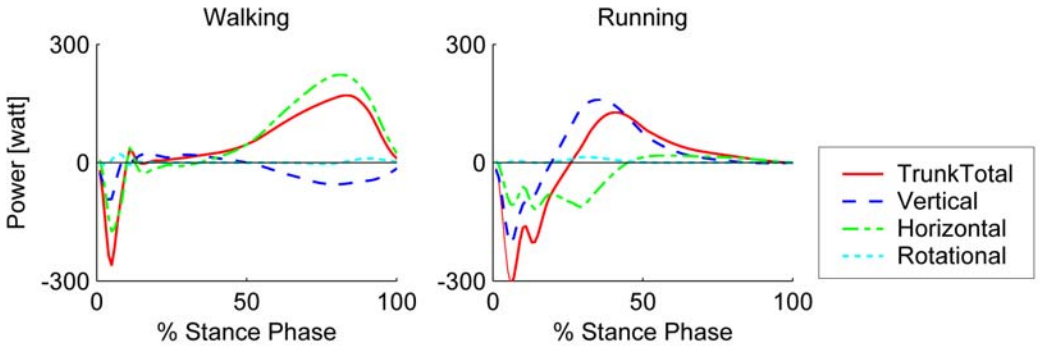

Fig. 2.7: Trunk power distributions by SOL

Trunk power distributions by SOL during stance in walking and running at the preferred transition speed. TrunkTotal: total trunk power generated by SOL; Vertical: trunk vertical kinetic power and potential power; Horizontal: trunk horizontal kinetic power; Rotational: trunk rotational power.

The bi-articular HAM did not show significant contributions to body support or forward progression during stance in both walking and running at the PTS (except in the beginning of stance in walking). However, previous studies have suggested that HAM play a major role in running, especially at higher speeds (e.g., Mann and Sprague, 1980; Belli et al., 2002). Kyrolainen et al. (1999) found that biceps femoris long-head had the largest increase in EMG activity among the muscles examined in their study as running speed increased from 3.25 m/s to the subjects' maximal speed. In the present study, HAM delivered power to the leg to accelerate the leg forward in both walking (from the beginning to mid-stance) and running (from mid- to late stance) (Fig. 2.4b: HAM, Walking, ~10-30% gait cycle, Running, ~20-40% gait cycle). A similar function has been observed in walking at self-selected speeds (Neptune et al., 2004a). The running simulation (at 1.96 m/s) showed that HAM generated a small amount of propulsive horizontal ground reaction force (Fig. 2.8: HAM, ~50-100% stance), which resulted in

accelerating the leg forward (Fig. 2.9: HAM, Horizontal, ~50-100% stance). Further investigation is needed to assess whether and how this functional role changes as running speed increases.

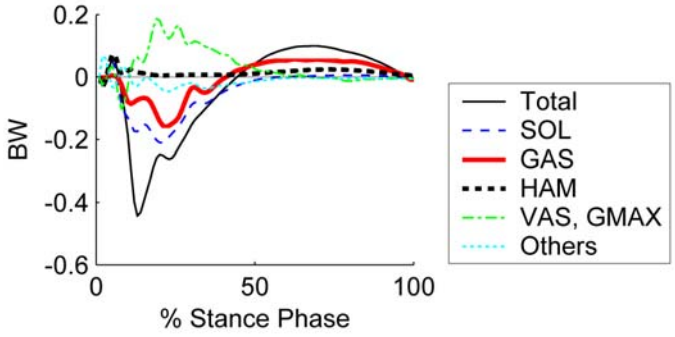

Fig. 2.8: Muscle contributions to hGRF

Muscle contributions to the horizontal ground reaction force in running at the preferred transition speed. Total: total horizontal ground reaction force; VAS, GMAX: VAS and GMAX combined; Others: all other muscles combined.

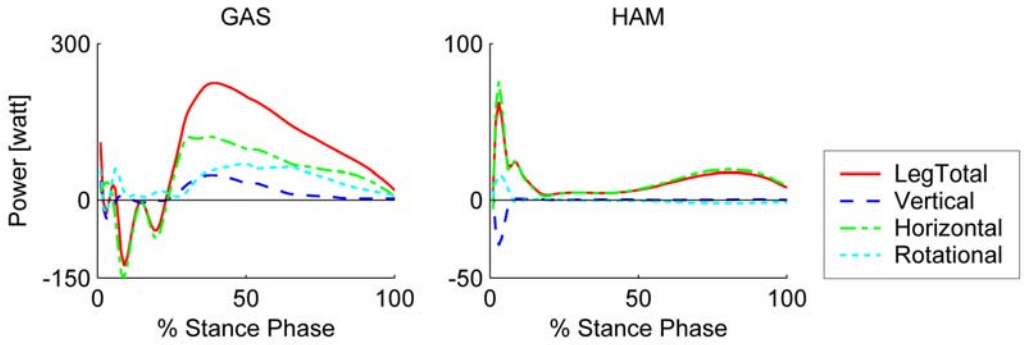

Fig. 2.9: Leg power distributions by GAS and HAM

Leg power distributions by GAS and HAM during stance in running at the preferred transition speed. LegTotal: total leg power generated by the muscles; Vertical: leg vertical kinetic power and potential power; Horizontal: leg horizontal kinetic power; Rotational: leg rotational power. Note that the scale is different for the two muscles to highlight the difference in power distributions.

Other muscles showed consistent patterns of body support, forward progression and body segmental power distributions during walking and running, which was independent of excitation timing or duration. For example, GAS peak activity occurred earlier in stance during running compared to walking (Fig. 2.3: GAS). However, the muscle functioned similarly to deliver power to the leg, and to a lesser degree, to the trunk in both walking and running during its peak activity (Fig. 2.4a: GAS). Eccentric RF action during the late stance that contributed to forward progression in walking (Fig. 2.5: RF, Horizontal, dashed line, ~80-100% stance, also Neptune et al., 2004a; Zajac et al., 2003) was negligible during the late stance in running. Instead, a small contribution to forward progression occurred from the beginning to mid-stance in synergy with VAS and GMAX (Fig. 2.5: RF, Horizontal, solid line, ~10-60% stance). However, RF segment power distribution patterns were essentially unchanged between walking and running (Fig. 2.4c: RF). VAS, GMAX and BFsh maintained similar contributions to body support, forward progression and power distributions in walking and running, although the contributions were increased in the magnitude and duration in running (Fig. 2.4b, 2.4c, 2.5: VAS, GMAX, BFsh). IL slightly decreased its mechanical power when switching from walking to running (Fig. 2.4c: IL), which would be explained by more flexed knee joint that would decrease the moment of inertia of the leg relative to the hip, and therefore require a lower hip flexion moment during swing in running (Grillner et al., 1979). However, the overall power distribution of the muscle was not altered. TA had negligible contribution to support and forward progression in both walking and running except in the beginning of stance (Fig. 2.5: TA).

Such similarities in muscle contributions to the task energetics between walking and running at the PTS suggest that partially similar neuromotor control strategies are used in the two locomotor tasks. The qualitative functional roles of the uni-articular

muscles at the hip and knee joints were nearly identical between walking and running. Previous EMG studies have suggested that the control strategies of hip flexors (iliacus and psoas), hip and knee extensors (gluteus maximus and vastus medialis/lateralis) during walking and running at the same speeds are relatively consistent (Andersson et al., 1997; Nilsson et al., 1985). Similarly, segmental kinematic analysis has also shown that the continuous relative phase (difference between thigh and shank angles) over a gait cycle in walking and running at the same speed and stride frequency is qualitatively similar (Li, 1999). Such similarities between gait modes would provide the basis for simplifying the control strategies of the muscles crossing the hip and knee joints.

The present study showed that in running VAS and GMAX contribution to forward progression primarily occurred from the beginning to mid-stance and then decreased toward late stance, and that SOL, GAS and other muscles made little contributions to forward progression. Consequently, the question arises concerning which muscle group is responsible for generating the propulsive horizontal GRF from mid- to late stance in running (Fig. 2.2: Running, hGRF, ~20-40% gait cycle). There have been inconsistencies among studies regarding the plantar flexors as a contributor to the propulsive horizontal GRF. Some studies have suggested that the primary contribution of the plantar flexors is to provide forward propulsion in the second half of the stance phase, in synergy with hip and knee extensors (e.g., Brandell, 1973; Simonsen et al., 1985; Novacheck, 1998), while others disagree, noting that plantar flexor activation ceases before toe-off (e.g., Mann et al., 1986; Reber et al., 1993). We found that GAS contributed the most among all muscles to the propulsive horizontal GRF (Fig. 2.8: GAS). GAS distributed most of its power to the leg during mid- to late stance (Fig. 2.4a: GAS, Running, ~15-40% gait cycle) to accelerate the leg horizontally rather than the trunk during the same period (Fig. 2.9: GAS Horizontal). In contrast, SOL had little

contribution to the propulsive horizontal GRF (Fig. 2.8: SOL). Previous studies have found that SOL activity is significantly lower than GAS in late stance (Reber et al., 1993) and that the duration of GAS activity is prolonged relative to SOL activity (Swanson and Caldwell, 2000). Such results are consistent with the differences in function of SOL and GAS, with SOL providing support in mid-stance and GAS contributing to propulsive horizontal GRF and swing initiation from mid- to late stance.

The differences in SOL and GAS contributions to propulsive horizontal GRF in running appear to be related to the knee joint angle in mid- to late stance. The contractile state of both muscles becomes more unfavorable to force generation in late stance (i.e., shortened muscle fiber length and increased concentric contraction velocity) because of increasing plantar flexion (Fig. 2.2: Running, Ankle, ~20-40% gait cycle). However, GAS is less susceptive to the change in the contractile state because the knee joint continues to extend during the same region (Fig. 2.2: Running, Knee, ~20-40% gait cycle), and therefore, more suitable for generating force to provide propulsive horizontal GRF than SOL (Fig. 2.8: SOL < GAS, ~50-100% stance). In contrast, in walking SOL has a more dominant role in providing forward progression over GAS in late stance (e.g., Neptune et al., 2001, also Fig. 2.5: SOL, GAS, Horizontal, dashed line, ~50-100% stance), which may reflect less favorable contractile state for GAS due to knee flexion that starts in late stance (Fig. 2.2: Walking, Knee, ~40-60% gait cycle).

In summary, our simulation analyses showed that when switching from a walk to a run at the preferred transition speed, the same muscle groups (the plantar flexors, VAS and GMAX) provided body support, while forward progression was provided primarily by VAS and GMAX with negligible contributions from the plantar flexors. SOL appeared to have the most distinctive differences in function between walking and running among all muscles examined. In running, SOL was activated earlier in the stance

phase to work in synergy with the hip and knee extensors to generate upward acceleration necessary for the subsequent flight phase. Other muscles showed qualitatively similar functional roles to distribute power and to provide body support and forward progression in both walking and running. In running, GAS, and to a lesser degree HAM, provided propulsive horizontal GRF that resulted in accelerating the leg rather than the trunk.

CHAPTER3

Muscle mechanical work and elastic energy utilization during walking and running near the preferred gait transition speed

INTRODUCTION

Muscle mechanical energy expenditure is an important quantity to analyze human locomotion since it reflects the neuromotor strategies used by the nervous system and is directly related to the efficiency of the task. Energy conservation is a characteristic of many common motor tasks and generally leads to a preferred mode in performing a given task (Sparrow et al., 2000). Previous studies have suggested that the two primary energy saving mechanisms in walking are the passive exchange of potential and kinetic energy (e.g., Cavagna and Margaria, 1966) and elastic energy utilization (e.g., Hof, 1990). Assuming that walking can be modeled as an inverted-pendulum, the theoretical efficiency of the energetic exchange between kinetic and potential energy (or energy recovery) is only as high as 65% and varies depending on walking speed (Cavagna et al., 1976) and stride frequency (Minetti et al., 1995). In addition, Neptune et al. (2004b) recently found that considerable muscle work is needed to produce the inverted pendulum-like motion. Thus, the passive energy exchange mechanism in normal walking may not be as significant as that observed in simple inverted-pendulum models.

Elastic energy utilization where mechanical energy is stored and released in tendons is considered to be an important metabolic energy saving mechanism, especially in running (e.g., Alexander, 1988; Hof, 1990). Potential and kinetic energy has the potential to be converted to elastic energy that is stored in compliant tendinous structures,

and subsequently released to do positive work at a later point in the gait cycle. The Achilles tendon of the ankle plantar flexors is one of the most widely studied structures, and previous studies have estimated that nearly 50% of the total mechanical energy of the body is stored in the Achilles tendon and the arch of the foot during the stance in running (Alexander and Bennet-Clark, 1977; Ker et al., 1987). Other tendons that are rapidly stretched during the loading response (e.g., knee extensor tendons) are also assumed to play an important role (Alexander, 1984).

Tendons not only store and return elastic energy, but also act to reduce the corresponding muscle fibers' shortening velocity to allow the fibers to operate at more favorable contractile state. The reduction in fiber velocity increases the fiber contraction efficiency and reduces the corresponding metabolic cost (Roberts, 2002). Such reductions in fiber velocities have been observed in distal extensor muscles *in vivo* in hopping/running animals (Roberts et al., 1997; Biewener et al., 1998) and humans during walking (Fukunaga et al., 2001). With the reduction of metabolic cost, tendon elastic energy storage and return has been put forth as an important determinant of the preferred gait mode (walking or running) at a given speed (Kram et al., 1997; Raynor et al., 2002). These studies have suggested that above the speed at which subjects prefer to run rather than walk (i.e., the preferred walk-to-run transition speed or PTS), running becomes metabolically more efficient because the tendon elastic energy storage and return can be utilized more effectively. Inversely, below the PTS the tendon elasticity utilization decreases, and therefore, walking is preferred. These differences in tendon elasticity utilization are assumed to be reflected in the lower metabolic cost associated with each preferred gait mode. The metabolic cost of running is lower than walking at speeds above the PTS, and inversely, running becomes more costly than walking at speeds below the PTS (e.g., Brisswalter and Mottet, 1996; Hanna et al., 2000), with the increased cost

related to an increase in muscle fiber work. However, no study has quantified the relative fiber to tendon work ratios in walking and running to test these hypotheses.

Previous studies have measured muscle force and length *in vivo* in a limited number of muscles in animals (Roberts et al., 1997; Biewener et al., 1998) and humans (e.g., Komi et al., 1992; Kyrolainen et al., 2003). Methodologically, force and length measurement *in vivo* is extremely difficult, either by surgically implanting force and length sensors into muscles (Roberts et al., 1997; Biewener et al., 1998) or using complex imaging techniques to obtain fiber lengths and estimating the corresponding musculotendon forces (e.g., Narici et al., 1996; Kawakami et al., 1998; Fukunaga et al., 2002). The complexity of such measurements has limited the number of muscles and conditions under which such measurements can be made. Rather than using direct measurements or imaging techniques, earlier studies had used traditional gait analysis techniques to compute changes in segmental mechanical energy (e.g., Cavagna and Kaneko, 1977; Winter, 1979; Caldwell and Forrester, 1992) as an indirect approach for estimating fiber and tendon work. However, these methods cannot account for co-contractions of antagonistic muscle groups and separate individual muscle fiber and tendon contributions to mechanical energy state of the system (Neptune and van den Bogert, 1998).

In contrast, forward dynamic simulations using musculotendon actuators that include tendon compliance can provide a powerful framework to quantify individual muscle contributions to the mechanical energetics of a given motor task (Neptune et al., 2004b; Zajac et al., 2003). Therefore, the overall goal of this study was to develop forward dynamic simulations of walking and running at speeds above and below the PTS to examine musculotendon mechanical work output and tendon elasticity utilization. Our specific objectives were to assess the premise that 1) fiber work is higher in walking than

running above the PTS, and inversely, higher in running than walking below the PTS, 2) the tendon elasticity utilization during stance is higher in running above the PTS than in running below the PTS, which would indicate that the tendon elastic energy store and return is more effective at higher speeds.

METHODS

1 Forward dynamics simulations

1.1 Musculoskeletal model

A sagittal-plane musculoskeletal model and forward dynamic simulations to emulate human walking and running above and below the preferred transition speed (PTS) were developed using SIMM (MusculoGraphics Inc.[1], Evanston, IL) and Dynamics Pipeline (MusculoGraphics Inc., Evanston, IL). The model consisted of a trunk (head, arms, torso and pelvis) and right and left legs (femur, tibia, patella, and foot). The dynamic equations of motion for the system with nine degrees-of-freedom (hip, knee, ankle flexion and extension for both legs, and trunk horizontal and vertical translation and rotation) were generated using SD/FAST (PTC Inc.[2], Needham, MA). The knee joint was defined using a planar joint, with prescribed translational motion of the tibia relative to the femur as a function of the knee angle (Yamaguchi and Zajac, 1989; Delp, 1990). The position and orientation of the patella relative to the tibia were prescribed in the similar manner (Yamaguchi and Zajac, 1989; Delp, 1990). Fifteen Hill-type musculotendon actuators per leg representing the major lower-extremity muscles were included in the model (Neptune at al., 2001, 2004a, b; Zajac et al., 2003). These muscles were combined into nine functional groups that received the same excitation signals based on anatomical classification. The groups were defined as: GMAX (gluteus maximus, adductor magnus), IL (iliacus, psoas), HAM (biceps femoris long head, medial hamstrings), VAS (3-component vastus), RF (rectus femoris), BFsh (biceps femoris short

[1] URL: http://www.musculographics.com/
[2] URL: http://www.ptc.com/

head), TA (tibialis anterior), GAS (medial and lateral gastrocnemius) and SOL (soleus). Each muscle's excitation was based on surface-EMG based signals (see *Experimental data collection* below). For the muscles in which surface EMG was not available (i.e., IL and BFsh), a block excitation pattern was used (e.g., Neptune et al., 2001, 2004a). The muscle excitation-activation dynamics was described using a first-order differential equation (Raasch et al., 1997) with activation and deactivation time constants of 5 and 10 ms, respectively. Passive torques representing the ligaments and other connective tissues were applied to each joint (Davy and Audu, 1987). The contact between the foot and ground was modeled using thirty visco-elastic elements attached to each foot segment (Neptune et al., 2000).

1.2 Dynamic optimization

Well-coordinated walking and running simulations over the gait cycle (i.e., from right foot-strike to right foot-strike) were generated by optimizing the EMG-based muscle excitation patterns to minimize the differences between the simulation and experimental kinematics and ground reaction forces (GRFs). (see *Experimental data collection* below). A simulated annealing algorithm (Goffe et al., 1994) was used in this dynamic tracking optimization to adjust the onset, offset and magnitude of the excitation patterns in the simulation (e.g., Neptune and Hull, 1998; Neptune et al., 2001; Zajac et al., 2003).

1.3 Mechanical work done by the muscle fibers and tendons

Positive, negative and total mechanical work done by the muscle fibers or tendons during the stance and swing phases was obtained by time-integration of muscle fiber or tendon power over the stance and swing phases of the gait cycle as:

$$\text{Mechanical work} = \int_{t_1}^{t_2} P dt \quad (3.1)$$

where P is the positive or negative power in the fiber or tendon, t_1 and t_2 define the duration of positive or negative power within the stance or swing phase.

The total fiber work was obtained by summing the positive and the absolute value of the negative fiber work over the gait cycle across all muscles. Similarly, the net fiber work was computed by summing the positive and negative fiber work.

The tendon elasticity utilization was defined as the ratio of the positive tendon to positive fiber work during each muscle's active region in the stance phase (i.e., when the muscle's active state was greater than 0.03) as:

$$\text{Tendon elasticity utilization} = 100 \times (\text{positive tendon work} / \text{positive fiber work}) \quad (3.2)$$

To assess the total elasticity utilization of all muscles, the same ratio was computed for the total positive tendon and total positive fiber work of all muscles in the stance phase.

2 Experimental data collection

Body segment kinematic, GRF and EMG data during walking and running above and below the PTS were collected from ten healthy subjects (5 males and 5 females: age

29.6 ± 6.1 years old, height 169.7 ± 10.9 cm, body mass 65.6 ± 10.7 kg). The two speeds examined were 80% and 120% of the subject's PTS, which are the speeds where the difference of metabolic cost between walking and running is clearly observed (e.g., Hanna et al., 2000). Informed consent approved by the Cleveland Clinic Foundation and The University of Texas at Austin was obtained from each subject before participating in the experiments. All data were collected at the Cleveland Clinic Foundation in Cleveland, OH.

2.1. Determining the preferred transition speed

Each subject's PTS was determined on a split-belt treadmill with embedded force plates (TecMachine[1], France). After warming up and becoming familiarized with the treadmill, each subject started walking at 0.6 m/s. Then, each subject was instructed to either walk or run while the treadmill speed was systematically increased by 0.1 m/s every 30 seconds. The stepped protocol was continued until the treadmill speed reached the point where the subject chose to run during the entire 30-second interval, which was defined as the PTS for that trial. Three trials were conducted and average-PTS was obtained.

2.2 Data acquisition and processing

The kinematic, GRF and EMG data were collected for 15 seconds at the sampling frequencies of 120, 480 and 1200 Hz, respectively, near the end of a randomly assigned one-minute trial of walking or running on the treadmill above and below the PTS. A three-minute-break was prescribed between trials. The kinematic data were captured

[1] URL: http://www.hef.fr/A20.HTML

using Motion Analysis system (Motion Analysis[1], Santa Rosa, CA). A modified Helen Hayes marker set (one-inch diameter reflective markers) was used to define body segments. The EMG data were collected from the right leg muscles. Disposable surface bi-polar EMG electrodes (Noraxon[2], Scottsdale, AZ) were attached to the following muscle bellies using the guidelines provided by Perotto (1994): the gluteus maximus, rectus femoris, vastus medialis, biceps femoris long head, medial gastrocnemius, soleus and tibialis anterior. All data were digitally filtered using fourth-order zero-lag Butterworth filters. The cut-off frequencies for the kinematic and GRF data were 6 and 20 Hz, respectively (e.g., Winter, 1990; Antonsson and Mann, 1985). EMG data were processed using band-pass filter (20-400 Hz), full rectification and low-pass filter (10 Hz) (e.g., Gonzalez et al., 1996). The resultant EMG linear envelopes were then normalized to each muscle's maximum value observed during the running trial above the PTS. All data were time-normalized to a full gait cycle, and were averaged within each subject and then across subjects to obtain group average data.

[1] URL: http://www.motionanalysis.com/
[2] URL: http://www.noraxon.com/

RESULTS

The group-average PTS was 1.96 ± 0.17 m/s, yielding simulations of walking and running at 1.6 and 2.4 m/s that corresponded to speeds of 80% and 120% of the PTS, respectively. Hereinafter, walking and running at the two speeds will be labeled as W80, W120, R80 and R120. The corresponding walking and running simulations emulated the experimental data almost always within ± 2 S.D. of the group-average (Fig. 3.1).

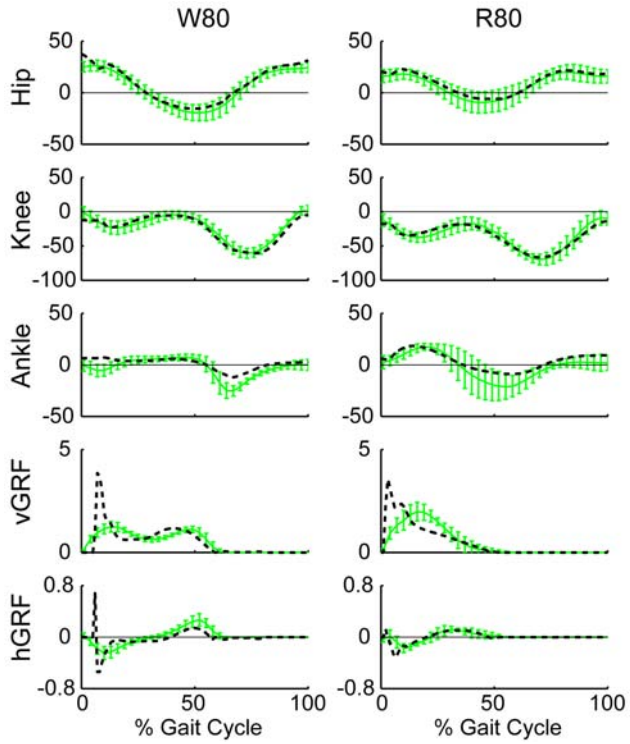

Fig. 3.1: Tracking results

Hip, knee and ankle joint angles (units: degrees) and vertical (vGRF) and horizontal (hGRF) ground reaction forces (units: normalized to body weight) in walking (W80) and running (R80) simulations (dashed line) and experimental data (solid line, average ± 2 S.D.). Positive angles indicate flexion, extension and dorsiflexion in the hip, knee and ankle joints, respectively. Similar tracking results were obtained for the 120% PTS walking and running conditions.

The muscle excitation timing compared well with the EMG patterns, assuring that muscle force was generated at the appropriate region of the gait cycle (Fig. 3.2).

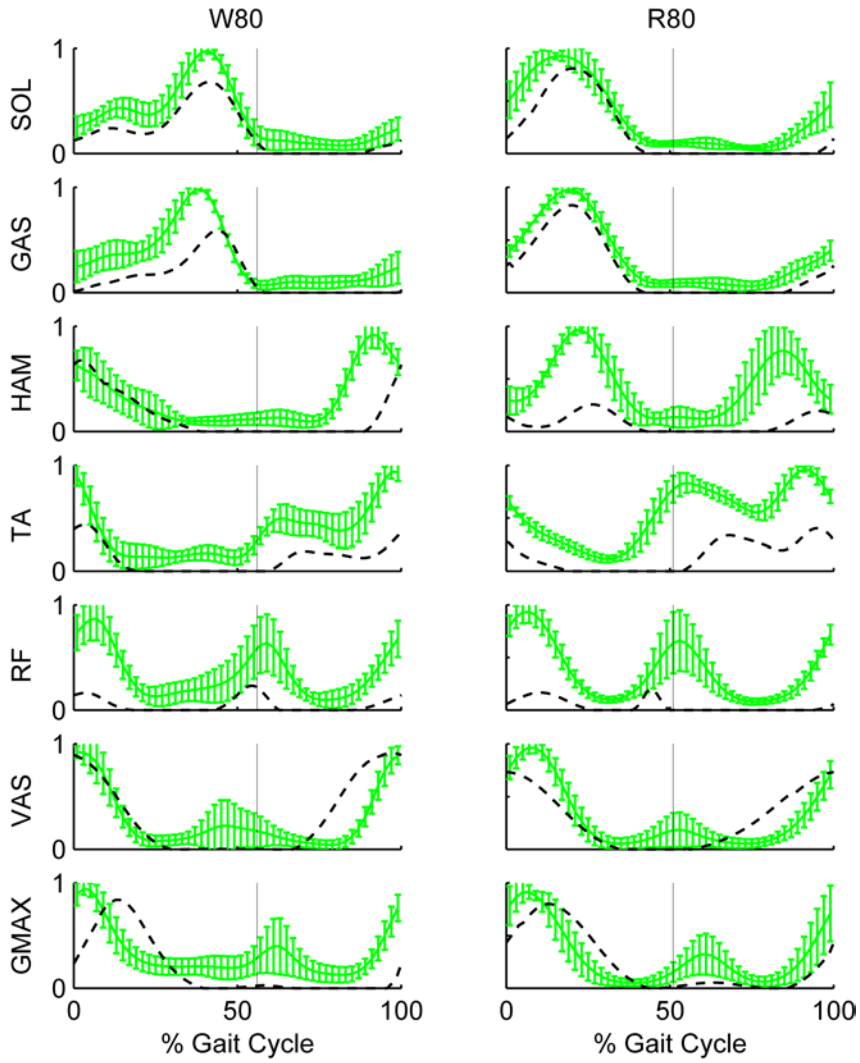

Fig. 3.2: Muscle excitation patterns

Muscle excitation patterns for the walking (W80) and running (R80) simulations (dashed line) and group average EMG linear envelopes (solid line, average ± S.D.). The EMG data were normalized to the maximum value observed over the gait cycle for each muscle. The vertical lines indicate toe-off.

Overall fiber and tendon mechanical work

The magnitude of fiber and tendon work was greater during stance than swing (Table 3.1). During stance, the positive work by plantar flexors (SOL and GAS) and GMAX, and negative work by VAS were significant. (Fig. 3.3: FiberNegative, FiberPositive). HAM also generated positive work to a lesser extent (Fig. 3.3: HAM, FiberPositive). Positive tendon work was significant in the plantar flexors and VAS, especially during running (Fig. 3.3: SOL, GAS, VAS, TendonPositive).

Table 3.1: Musculotendon mechanical work

Mechanical work (units: joules) done by all muscle fibers and tendons during stance, swing and over the gait cycle in walking (W) and running (R) at 80 % and 120 % PTS. The values in parentheses for fiber work represent passive fiber work. Work Ratio is the ratio of positive tendon work to positive fiber work during stance, which represents the tendon elasticity utilization.

		W80	R80	W120	R120
Fiber Stance					
	Positive	44 (3)	59 (2)	65 (3)	57 (2)
	Negative	28 (6)	52 (4)	50 (6)	57 (3)
Fiber Swing					
	Positive	26 (6)	25 (5)	45 (8)	45 (7)
	Negative	15 (5)	18 (4)	32 (6)	30 (7)
Fiber Total		**113**	**154**	**192**	**189**
Fiber Net		**27**	**13**	**29**	**15**
Tendon Stance					
	Positive	23	27	25	45
	Negative	17	21	19	40
Tendon Swing					
	Positive	2	3	8	5
	Negative	4	5	8	10
Positive Tendon Work Total		**25**	**30**	**33**	**50**
Work Ratio (%)		**52**	**45**	**39**	**79**

During swing, muscle fiber work was produced primarily by HAM (negative work), TA (positive), VAS (positive) and IL (positive) (Fig. 3.4: HAM, TA, VAS, IL, FiberPositive, FiberNegative). Very little tendon work occurred during swing. Only a small amount of tendon work was observed in HAM and RF at W120 (Fig. 3.4: HAM, RF, TendonPositive).

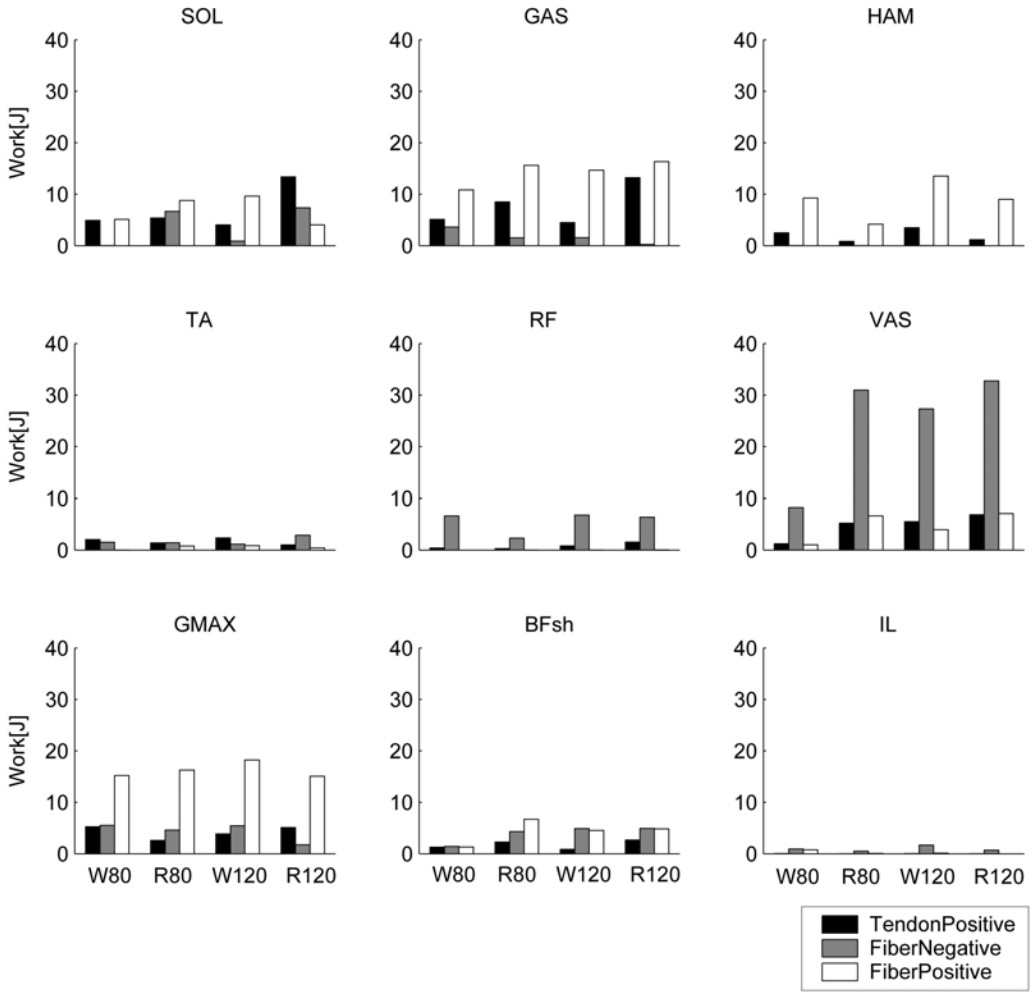

Fig. 3.3: Mechanical work during stance

Mechanical work done by individual tendons and fibers during stance in walking (W) and running (R) at 80 % and 120% PTS.

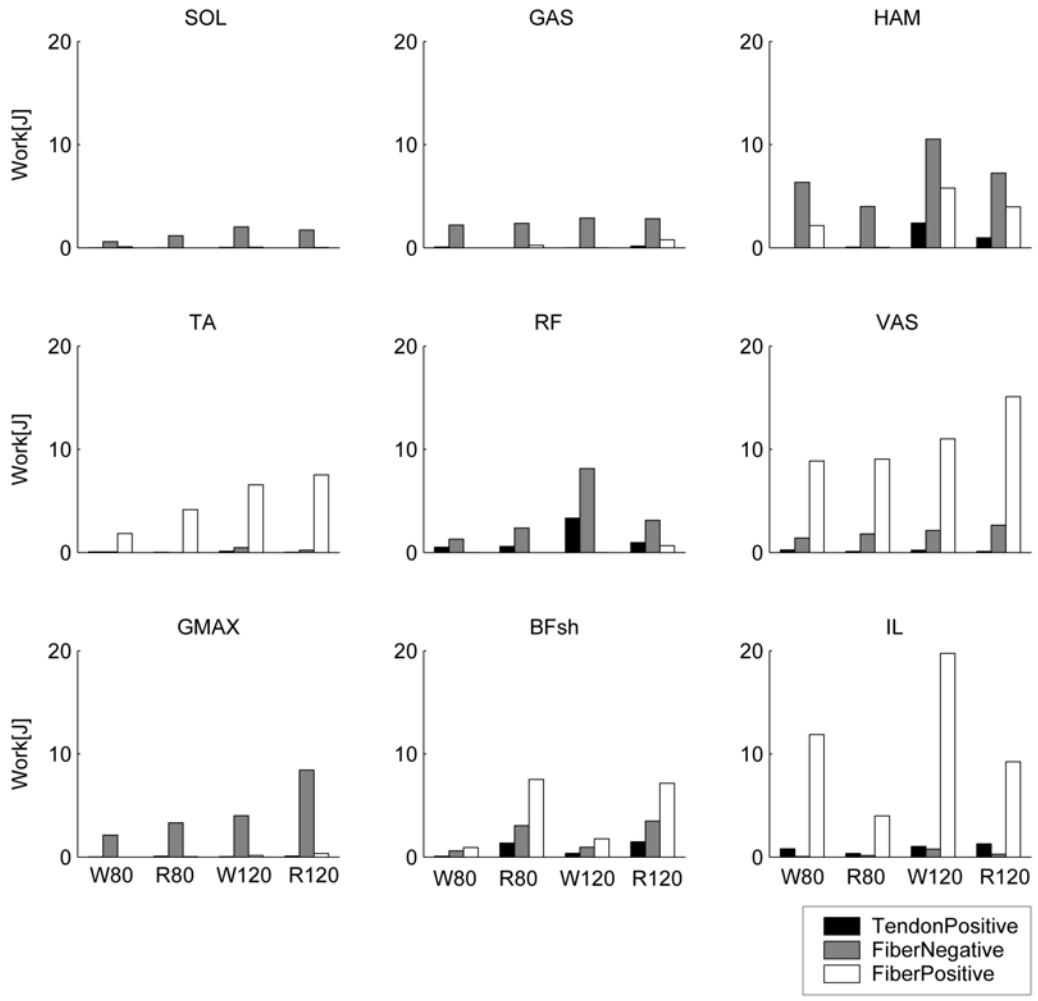

Fig. 3.4: Mechanical work during swing

Mechanical work done by individual tendons and fibers during swing in walking (W) and running (R) at 80 % PTS and 120% PTS.

Comparison between W80 and R80

The total fiber work done by the muscles was 41 J greater in running than in walking (Table 3.1: Fiber Total W80 and R80). The difference was primarily attributed to an increase in VAS negative work in stance during running (~22 J) (Fig. 3.3: VAS, FiberNegative, W80 and R80). Increased work was also observed in the plantar flexors and BFsh (Fig. 3.3: SOL, GAS, BFsh, FiberNegative, FiberPositive, W80 and R80). The positive fiber work during swing was similar in both gaits (26 J and 25 J, Table 3.1: W80 and R80), although differences were observed in IL and BFsh that offset each other. The IL contribution was larger in walking than running (~8 J difference), while the BFsh contribution was larger in running than walking (~7 J difference) (Fig. 3.4: IL, BFsh, FiberPositive, W80 and R80). The total positive work done by all tendons was slightly higher in running than in walking (Table 3.1: Positive Tendon Work Total, W80 and R80), with the difference due primarily to GAS and VAS (~ 4 J each) (Fig. 3.3: GAS, VAS, TendonPositive). The tendon elasticity utilization was greater in W80 than R80 due to the lower fiber work required at W80 (Table 3.1: Work Ratio, W80 and R80).

Comparison between W120 and R120

The total muscle fiber work decreased slightly when switching from walking to running at 120% PTS (Table 3.1: Fiber Total, W120 and R120). During stance, VAS increased both positive and negative work (~ 5 J and 3 J, respectively) (Fig. 3.3:VAS, FiberPositive, FiberNegative, W120 and R120), while SOL, HAM and GMAX positive work decreased (~ 4 J each) (Fig. 3.3: SOL, HAM, GMAX, FiberPositive, W120 and R120). Although positive and negative fiber work during swing was similar between the gaits (Table 3.1: Fiber Swing, W120 and R120), marked decreases in IL positive work (~ 11 J) and to a lesser degree in RF negative work (~ 5 J) and HAM positive and negative

work (~ 2 and 5 J, respectively) were observed in running (Fig. 3.4: IL, RF, HAM, FiberNegative, FiberPositive). These decreases in fiber work were offset by an increase in work by VAS (positive: ~ 4 J), GMAX (negative: ~ 4 J) and BFsh (positive: ~6 J, negative: ~ 3 J) (Fig. 3.4: VAS, GMAX, BFsh, FiberNegative , FiberPositive), resulting in the similar total fiber work during swing. The total positive tendon work differed considerably between the two gaits, with greater positive tendon work (17 J) being done during the stance phase in running (Table 3.1: Positive Tendon Work, W120 and R120). This increase was primarily due to increased plantar flexor tendon work (Fig. 3.3: SOL, GAS, TendonPositive). The large increase in tendon work resulted in greater tendon elasticity utilization in running than walking above the PTS (Table 3.1: Work Ratio, W120 and R120).

DISCUSSION

The overall goal of this study was to examine musculotendon mechanical work and tendon elasticity utilization during both walking and running above and below the preferred transition speed (PTS). We hypothesized that fiber mechanical work in running is greater than the work in walking below the PTS, and inversely, that fiber work in running is lower than the work in walking above the PTS. We also hypothesized that tendon elasticity utilization (i.e., the ratio of tendon to fiber positive work during stance) is greater in running above the PTS than in running below the PTS.

Our simulation results support these hypotheses. The simulation data showed that the total fiber work in running below the PTS was ~36 % greater than in walking at the same speed, primarily due to greater stance-phase work (Table 3.1: Fiber Total, W80 vs. R80). In contrast, walking above the PTS showed slightly higher fiber work than running (Table 3.1: Fiber Total, W120 vs. R120). Thus, walking required less fiber work than running below the PTS and marginally higher fiber work above the PTS. This marginal difference in fiber work above the PTS was consistent with the study by Mercier et al. (1994), showing that the difference in metabolic cost between walking and running above the PTS (cost in walking > cost in running) tends to be smaller than the cost difference below the PTS (running > walking). Although we did not differentiate the relative cost difference between concentric and eccentric work (eccentric contraction consumes less metabolic energy than concentric contraction, e.g., Curtin and Davies, 1975), the trend of fiber mechanical work should follow the metabolic cost (e.g., Brisswalter and Mottet, 1996; Hanna et al., 2000) since the total positive (concentric) and negative (eccentric) fiber work were both greater in R80 than W80, and the difference in total positive work

between W120 and R120 (8 J, W120 > R120) was larger than the difference in the total negative work (5 J, W120 < R120).

The increase in fiber work in running compared to walking below the PTS (41 J, Table 3.1: Fiber Total) was primarily due to the increase in VAS eccentric work during stance (~ 24 J, Fig. 3.3: VAS FiberNegative, W80 and R80). The VAS work increase was due to greater knee flexion (Fig. 3.1: Knee, 0-20% gait cycle, W80 and R80) and larger force output in running (e.g., the peak values in walking and running were ~ 1600 N and ~3700 N, respectively). In contrast, the higher fiber work in walking compared to running above the PTS (3 J, Table 3.1: Fiber Total) was due to an increase in fiber work in HAM, RF and especially IL during swing phase (Fig. 3.4: HAM, RF, IL FiberNegative, FiberPositive, W120 and R120). The greater work in IL during swing in walking may be related to the increased demand on the hip flexors to overcome larger moment of inertia of the leg due to more extended knee joint during swing in walking (Grillner et al., 1979). Slightly greater IL mechanical power in walking was also observed at the PTS (see Chapter 2). The IL concentric action to accelerate the hip into flexion in early swing (Neptune et al., 2004a) appears to be much more pronounced when walking at higher speeds, which is consistent with EMG activity using fine wire-electrodes (Andersson et al., 1997). Thus, increased IL work during swing is potentially a disadvantage of walking above the PTS.

The simulation results also showed that significant fiber work occurs during swing in both walking and running at the speeds analyzed. For example, the net fiber work during the swing phase at W80 and R80 was ~40% and 54% of the net fiber work over the gait cycle, respectively (Table 3.1). Traditionally, studies have suggested that force production in the stance-leg is the primary determinant of the metabolic cost (e.g., Taylor et al., 1980; Kram and Taylor, 1990). However, recent analysis of metabolic

energy expenditure in running birds has revealed that the cost of swinging the leg is ~ 26 % of the total energy expenditure (Marsh et al., 2004). Further investigation is needed to measure metabolic cost associated with swinging the leg in human gait.

Running has historically been considered a "bouncing" gait that utilizes elastic energy stored and released in elastic tendons primarily during the stance phase (e.g., Alexander, 1988; Ker et al., 1987). Effective utilization of this elastic energy has been suggested as an important determinant of a preferred gait mode at a given speed (e.g. Kram et al., 1997; Raynor et al., 2002). The tendon elasticity utilization was quantified as the ratio of tendon to fiber positive work during the stance phase in the present study, which was shown to be much higher in running above the PTS than below the PTS (79 % vs. 45 %, Table 3.1: Work Ratio, R120 and R80). Thus, running below the PTS does not effectively use tendon elastic energy. This relative decrease in tendon work during running below the PTS may suggest that force required during slow running is not high enough to stretch the tendons. Indeed, our simulation showed that the peak force output in SOL and GAS (i.e., those muscles that exhibit the greatest tendon work in running, Fig. 3.3) was ~50 and ~25 % lower in R80 than R120, respectively. In contrast, the difference in musculotendon excursion between the two speeds during the loading response was less than 10% in both SOL and GAS. In addition, the relative tendon work decrease may also indicate the need for more precise and different neuromotor control that is not required during running above the PTS, which uses more tendon elasticity. Seyfarth et al. (2002) used a spring-mass running model to analyze how leg adjustments during running (i.e., altered leg stiffness and angle of attack) influences stability in running. Their results showed that as running speed decreases, the leg adjustment becomes more critical for stability, and that the spring-mass system needs to be operated above a certain speed to maintain a stable gait. These results suggest that running below

the PTS may not be a stable bouncing gait, and therefore, requires more control from muscle fibers. Biewener and Roberts (2000) suggested that muscles with a longer tendon and shorter fibers could save metabolic cost at the expense of accurate control of musculotendon length, and inversely, saving energy expenditure might be compromised by precise length control in a muscle with longer fibers and a shorter tendon. Such trade-offs between control and efficiency in muscles with different architecture may also be possible by an adjustment of force output in specific muscle groups.

Elastic energy storage and return occurred primarily in SOL and GAS, and to a lesser degree in VAS during stance (Fig. 3.3: SOL, GAS, VAS, TendonPositive). In SOL and GAS, the tendon elasticity utilization was much greater in running above the PTS than in running below the PTS (Fig. 3.5: R80 and R120). These results are consistent with previous studies showing that distal muscles with longer tendons in animals contract mostly in an isometric manner during stance in running (e.g., Roberts et al., 1997, Biewener et al., 1998). We also found that the elasticity utilization at W120 was substantially lower than R120 in SOL and GAS (Fig. 3.5: SOL, GAS, W120 and R120).

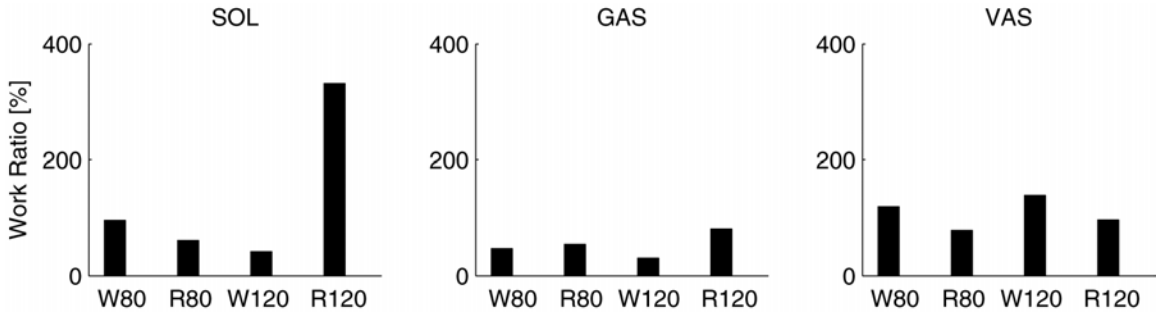

Fig. 3.5: Tendon elasticity utilization

The tendon elasticity utilization in SOL, GAS and VAS during each muscle's active region in the stance phase (i.e., when the muscle's active state was greater than 0.03) in walking (W) and running (R) at 80 % PTS and 120 % PTS.

The lower work ratio in these muscles in walking above the PTS may be related to low tendon shortening velocity relative to fiber velocity at that speed, since one of the important roles of the tendon is to reduce fiber shortening velocity to allow the fiber to operate effectively (Roberts, 2002). We performed a post-hoc analysis to obtain the ratio of tendon to fiber average shortening-velocity during the muscle's active region (i.e., muscle activation > 0.03) in the stance phase for SOL and GAS. The velocities of the tendon and fiber were obtained separately during the region, and then averaged within each region. The ratio showed that in walking above the PTS, the average fiber velocity in SOL and GAS was higher than the tendon velocity, indicating that the tendon does not reduce the fiber velocity (Fig. 3.6: SOL, GAS, W120 and R120).

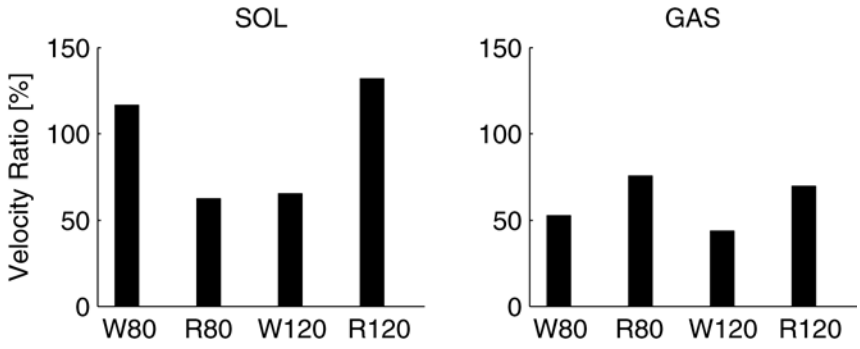

Fig. 3.6: Ratio of tendon to fiber average shortening velocity

The ratio of tendon to fiber average shortening velocity in SOL and GAS during each muscle's active region in the stance phase (i.e., when the muscle's active state was greater than 0.03) in walking (W) and running (R) at 80 % PTS and 120 % PTS.

Since the muscles' concentric contraction in late stance provides essential support and forward progression during walking (Neptune et al., 2001), the decreased effect of tendon

on reducing fiber velocity in SOL and GAS at higher walking speed is detrimental to force production. These findings are consistent with the results in Chapter 1, which showed that plantar flexor force production is impaired at higher walking speeds due to adverse fiber contractile conditions (i.e., fiber length and velocity). Thus, inefficient plantar flexor contraction appears to be a critical disadvantage of walking above the PTS.

Previous studies have suggested that TA, HAM and RF muscle activity in swing is closely related to important determinants of the preferred transition from walking to running (Hreljac, 1995a; Prilutsky and Gregor, 2001). The present study showed that HAM and RF fiber work during swing decreased when switching from a walk to run above the PTS (Fig. 3.4: HAM, RF, FiberNegative, FiberPositive, W120 and R120) and that TA fiber work did not differ much between walking and running at that speed. Thus, walking above the PTS is indeed disadvantageous for HAM and RF. However, the contractile state of HAM and RF (and TA) during swing has been found to be not as unfavorable for force production as the plantar flexors during stance in walking at higher speeds (see Chapter 1). Therefore, HAM, RF or TA contraction during swing does not appear to be a critical disadvantage in walking above the PTS.

Due to the limited number of experimental studies on fiber and tendon work, the comparison between empirically measured tendon work and the present study is only possible in the Achilles tendon. Alexander and Bennet-Clark (1977) and Ker et al. (1987) estimated the elastic energy storage in the Achilles tendon during running. Ker et al. (1987) showed that the tendon stores approximately 35 J during stance when running at 4.5 m/s. Force-length data measured *in vivo* by Kyrolainen et al. (2003) showed that approximately 17 J was stored in the tendon during running at 3 m/s (linear approximation was used in their force-length curve). Hof et al. (2002) indirectly estimated the musculotendon work using an inverse dynamics approach and showed that

during slow running (2.68-3.93 m/s), tendon work varied from ~10 J to ~39 J. These results are consistent with our simulation data showing that during running at 2.4 m/s (i.e., R120), the plantar flexor tendons returned ~ 27 J during stance (Fig. 3.3: SOL, GAS, TendonPositive, R120).

The limitations of the musculoskeletal model have been previously discussed in the studies using a similar model (Neptune et al., 2001, 2004a, b; Zajac et al., 2003; see also Chapter 1 and 2). In the present study, an additional potential limitation is that the tendon force-length relationship could alter the amount of fiber work and tendon elasticity utilization. To assess this possibility, we performed sensitivity analyses by changing the tendon stiffness by ± 20% for all muscles in the model. As expected, the magnitude of fiber and tendon work was altered, although our conclusions remained the same. For example, the combined positive tendon work by SOL and GAS during stance at R120 was 19 J and 29 J when the stiffness was increased (+20%) and decreased (–20%), respectively. However, the overall trend of fiber work and tendon elasticity utilization was not altered (Tables 3.2, 3.3). A second potential limitation is that fiber and tendon work could be affected by the rigid foot model. As Ker et al. (1987) estimated, the arch of the foot stores elastic energy (~ 17 J during running at 4.5 m/s). Therefore, excluding a compliant foot could result in overestimation of the musculotendon work. On the other hand, excluding the metatarso-phalangeal joint in the model could cause underestimation of the musculotendon work, since the joint absorbs (and does not return) mechanical energy (~ 21 J during running at 4 m/s, Stefanyshyn and Nigg, 1997). Consequently, excluding both structures may result in an offset of their influence on the musculotendon work. Further research is needed to assess this possibility.

Table 3.2: Musculotendon mechanical work (high tendon stiffness)

Mechanical work (units: joules) done by muscle fibers and tendons during stance, swing and over the gait cycle in walking (W) and running (R) at 80 % and 120 % PTS, when tendon force value was *increased* by 20 % for given length (i.e., stiffer tendon). The values in parentheses for fiber work represent passive fiber work. Work Ratio is the ratio of positive tendon work to positive fiber work during stance, which represents the tendon elasticity utilization.

		W80	R80	W120	R120
Fiber Stance					
	Positive	47 (3)	60 (2)	66 (3)	61 (2)
	Negative	27 (6)	54 (4)	55 (6)	64 (4)
Fiber Swing					
	Positive	30 (8)	25 (5)	46 (8)	30 (7)
	Negative	16 (5)	18 (4)	33 (6)	24 (7)
Fiber Total		**120**	**158**	**199**	**179**
Fiber Net		**34**	**13**	**24**	**4**
Tendon Stance					
	Positive	20	25	23	33
	Negative	15	19	17	28
Tendon Swing					
	Positive	2	3	7	3
	Negative	4	5	9	6
Positive Tendon Work Total		**22**	**28**	**30**	**36**
Work Ratio (%)		**43**	**41**	**35**	**54**

Table 3.3: Musculotendon mechanical work (low tendon stiffness)

Mechanical work (units: joules) done by muscle fibers and tendons during stance, swing and over the gait cycle in walking (W) and running (R) at 80 % and 120 % PTS, when tendon force value was *decreased* by 20 % for given length (i.e., more compliant tendon). The values in parentheses for fiber work represent passive fiber work. Work Ratio is the ratio of positive tendon work to positive fiber work during stance, which represents the tendon elasticity utilization.

		W80	R80	W120	R120
Fiber Stance					
	Positive	44 (3)	56 (2)	71 (5)	56 (1)
	Negative	24 (6)	51 (4)	64 (6)	52 (3)
Fiber Swing					
	Positive	32 (8)	25 (5)	42 (6)	31 (6)
	Negative	18 (5)	18 (4)	22 (5)	23 (6)
Fiber Total		**118**	**150**	**199**	**162**
Fiber Net		**35**	**13**	**28**	**13**
Tendon Stance					
	Positive	24	31	33	50
	Negative	20	25	25	42
Tendon Swing					
	Positive	3	3	5	8
	Negative	5	7	9	10
Positive Tendon Work Total		**27**	**34**	**38**	**58**
Work Ratio (%)		**54**	**55**	**46**	**89**

In summary, we found that fiber work in walking was lower than in running below the PTS, and inversely, the fiber work in walking was slightly higher than in running above the PTS, which was consistent with the metabolic cost of walking and running near the PTS (e.g., Brisswalter and Mottet, 1996; Hanna et al., 2000). Running below the PTS is not an efficient gait mode due to a decrease in tendon elasticity utilization and the increased fiber work required, and therefore, walking is a more suitable gait mode below the PTS. In contrast, running above the PTS is more efficient due to the less fiber work required than in walking and increased tendon elasticity utilization. The disadvantages of walking above the PTS include greater overall fiber work demands and corresponding metabolic cost, and increased fiber shortening velocity in the plantar flexors. These disadvantages make running a more suitable gait mode above the PTS.

CONCLUSION

SUMMARY

The primary goal of this study was to identify potential muscular determinants of the preferred walk-run gait transition in human gait. Forward dynamic simulations that emulated human walking and running at different speeds were used to analyze individual muscle groups in the lower extremities near the preferred gait transition speed (PTS). The analyses included clarifying the influence of intrinsic muscle properties (Chapter 1) and muscle fiber-tendon interactions (Chapter 3) on the gait transition and identifying differences in muscle function between walking and running at the PTS (Chapter 2).

The analysis of the influence of intrinsic properties on force generation in individual muscles revealed that force output in the ankle plantar flexors started to decrease despite a continuous increase in muscle activity as walking speed approached the PTS. The decrease in the force production was attributed to adverse contractile conditions (i.e., fiber length and velocity) during the propulsion phase as walking speed increased. The other major muscles increased their force production as muscle activation increased with walking speed, which was due to more favorable contractile conditions than the plantar flexors. Considering the important role of the plantar flexors in providing body support and forward progression in late stance during walking (Neptune et al., 2001), the impaired force production at the higher walking speeds was deemed an important determinant of the preferred walk-to-run transition speed.

With a transition to running at the PTS, the plantar flexor force and power output increased. However, their contribution to forward progression became negligible due to the different task mechanics of running, while their contribution to body support

remained unchanged. The soleus combined with the hip and knee extensors provided the necessary trunk upward acceleration for the subsequent flight phase. Although the plantar flexors did not contribute to forward progression in running, the gastrocnemius acted to accelerate the leg forward, thus providing the propulsive horizontal ground reaction force during mid- to late stance. In contrast, power generated by the soleus was directed upward in the trunk near mid-stance, and had little effect on leg acceleration. These differences observed in the soleus, combined with the decrease in soleus contribution to forward progression in running, were the most distinctive differences in muscle function between walking and running in all the major muscles examined. In the other muscles, the biomechanical function was qualitatively unaltered. These results suggest that the neuromotor control strategies when switching from walking to running may be simplified since the functional roles of most muscles are preserved between the two gait modes.

The analysis of mechanical work and tendon elasticity utilization between walking and running above and below the PTS revealed the advantages of each gait mode at a given speed. The total fiber work was lower in walking below the PTS and in running above the PTS. These results are consistent with measurements of metabolic cost in walking and running at different speeds near the PTS (e.g., Brisswalter and Mottet, 1996, Hanna et al., 2000). In addition, tendon elasticity utilization was higher in running above the PTS than in running below the PTS, indicating that running at higher speeds uses elastic energy return more effectively. These results provide insight into why walking below the PTS and running above the PTS are the preferred gait modes.

These series of three studies have provided much insight into potential muscular determinants of the preferred walk-run transition speed and why particular gait modes are preferred at a given speed.

FUTURE WORK

Developing 3-D forward dynamic gait simulations

The forward dynamic simulation analyses in this study revealed important biomechanical muscle functions during walking and running at or near the PTS. However, these simulations were constrained to the sagittal plane, which may potentially influence muscle function, particularly in those muscles that cross the hip joints (e.g., Neptune et al., 2004a). Thus, future work should be directed toward developing three-dimensional models with increased degrees-of-freedom at the appropriate joints. This may also help reduce the impact peak of the ground reaction forces observed in this study. For example, the hip adduction relative to the pelvis during stance has been suggested as a shock absorbing mechanism (Novacheck, 1998).

Other studies have used 3-D musculoskeletal models in simulation analyses (e.g., Anderson, 1999, Carhart, 2000). However, these models are not without shortcomings. For example, the walking simulation developed by Anderson (1999) using a 3-D musculoskeletal model possessing 23 degrees-of-freedom was able to reproduce the salient features of human walking at 1.36 m/s. However, an enormous amount of computational time was needed to optimize the muscle excitation patterns and produce a successful simulation. A "pseudo-inverse optimization" algorithm presented by Yamaguchi et al. (1995) was used to reduce the computational cost to generate a 3-D human walking simulation with 18 degrees-of-freedom (Carhart, 2000). However, the position of the center-of-pressure in the stance foot needed to be prescribed accurately in the optimization process, which may have affected the simulation and optimization performance.

Implementing closed-loop control

Three-dimensional walking simulations become more computationally feasible with the addition of feedback control. Currently, generating forward dynamic simulations is extremely difficult because the model control inputs (i.e., muscle excitations) are feed-forward. This open-loop system requires many iterations in the dynamic optimization to generate a stable walking pattern. In the present study, typically ~5000 iterations (~2000-3000 minutes) were needed to generate a satisfactory simulation. Future work should be directed toward integrating closed-loop feedback control algorithms. For example, Thelen et al. (2003) presented a "computed muscle control" algorithm that generated a pedaling simulation using a musculoskeletal model with 30 muscles and 3 degrees-of-freedom in ~10 minutes using a personal computer. However, the applicability of this algorithm to a less stable system (e.g., walking or running) remains to be determined.

Reducing the computational time to generate 3-D simulations of walking and running would allow us to investigate the influence of different musculoskeletal parameters among healthy and impaired individuals, and differences in muscle function during a variety of gaits (e.g., different gradients, directions and surfaces). Such investigations would extend the present work and our understanding of how individual muscles contribute to satisfying different task requirements during various types of gait, with the long-term goal of benefiting those individuals who are in need of effective rehabilitation strategies.

Appendix 1

(Each subject's preferred transition speed)

Table A1.1: The preferred transition speed of the subjects (S1-S10)

S1	S2	S3	S4	S5	S6	S7	S8	S9	S10	Average ± S.D.
1.72	1.89	1.61	2.11	2.05	2.05	2.11	2.11	2.00	1.94	1.96 ± 0.17

units: m/s

Appendix 2

(Experimental kinematic and GRF data of individual subjects)

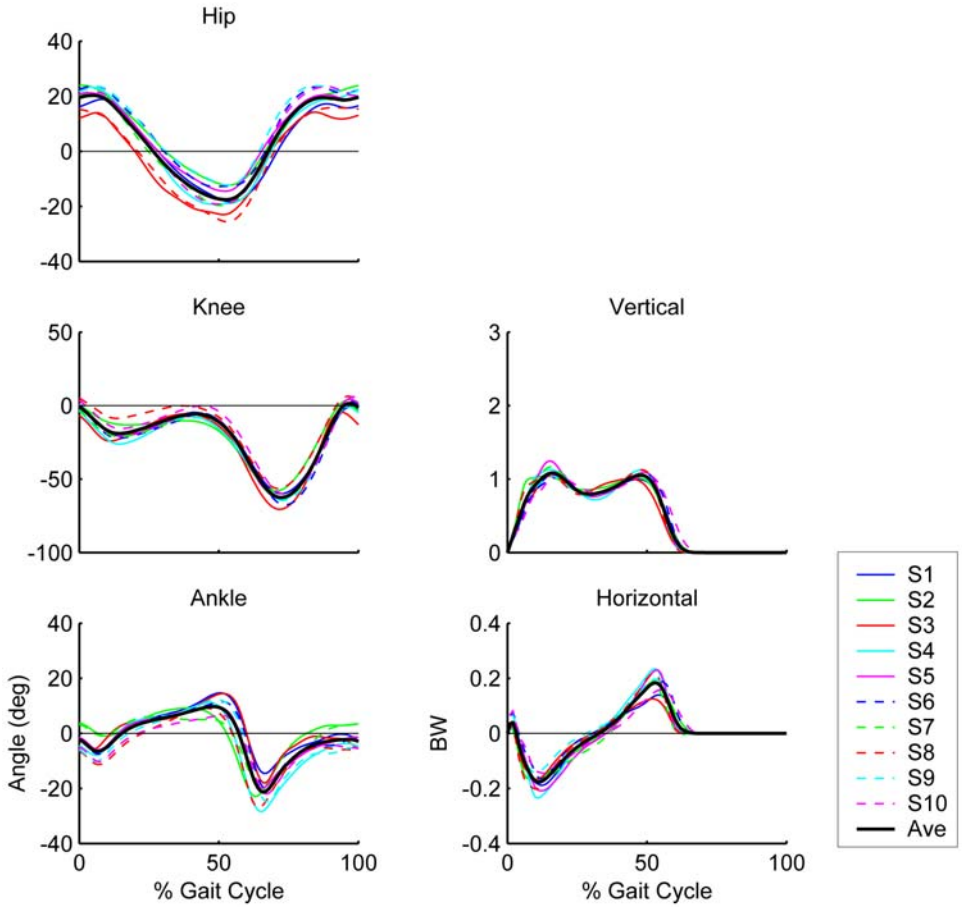

Fig. A2.1: Ensemble and group average kinematic and GRF data in W60

Hip, knee and ankle joint angles and vertical and horizontal ground reaction forces in walking at 60% PTS in ten subjects (S1-S10) and group average data (thick solid line).

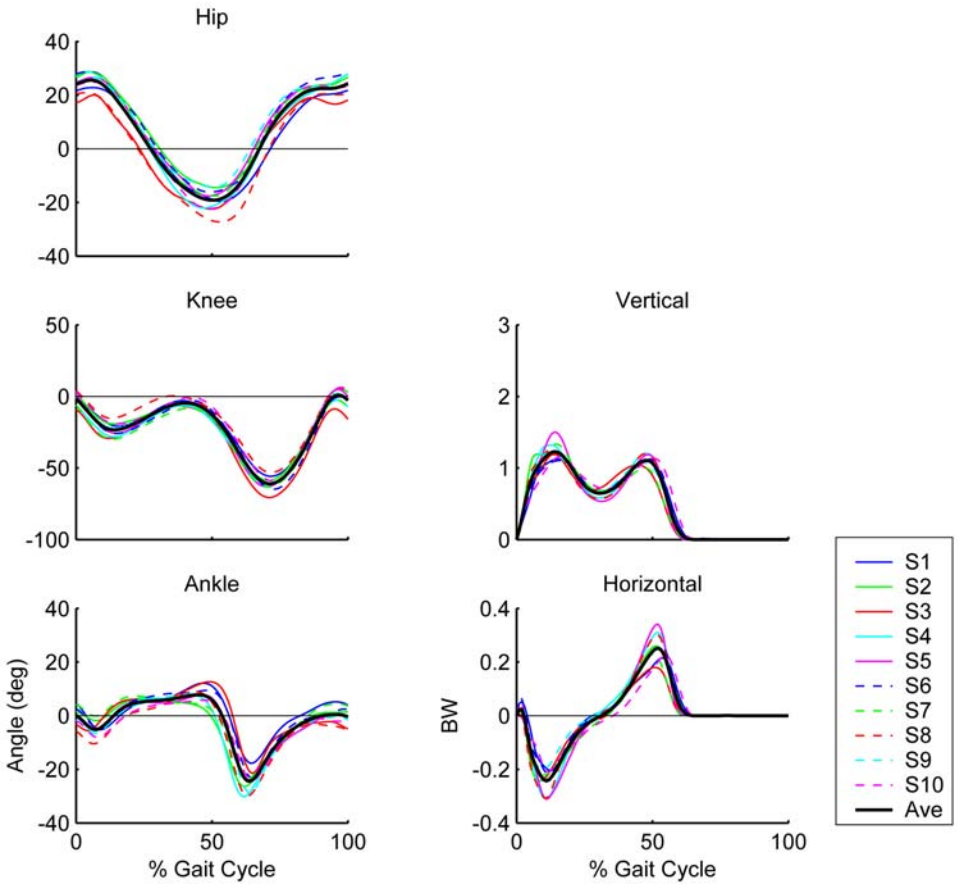

Fig. A2.2: Ensemble and group average kinematic and GRF data in W80

Hip, knee and ankle joint angles and vertical and horizontal ground reaction forces in walking at 80% PTS in ten subjects (S1-S10) and group average data (thick solid line).

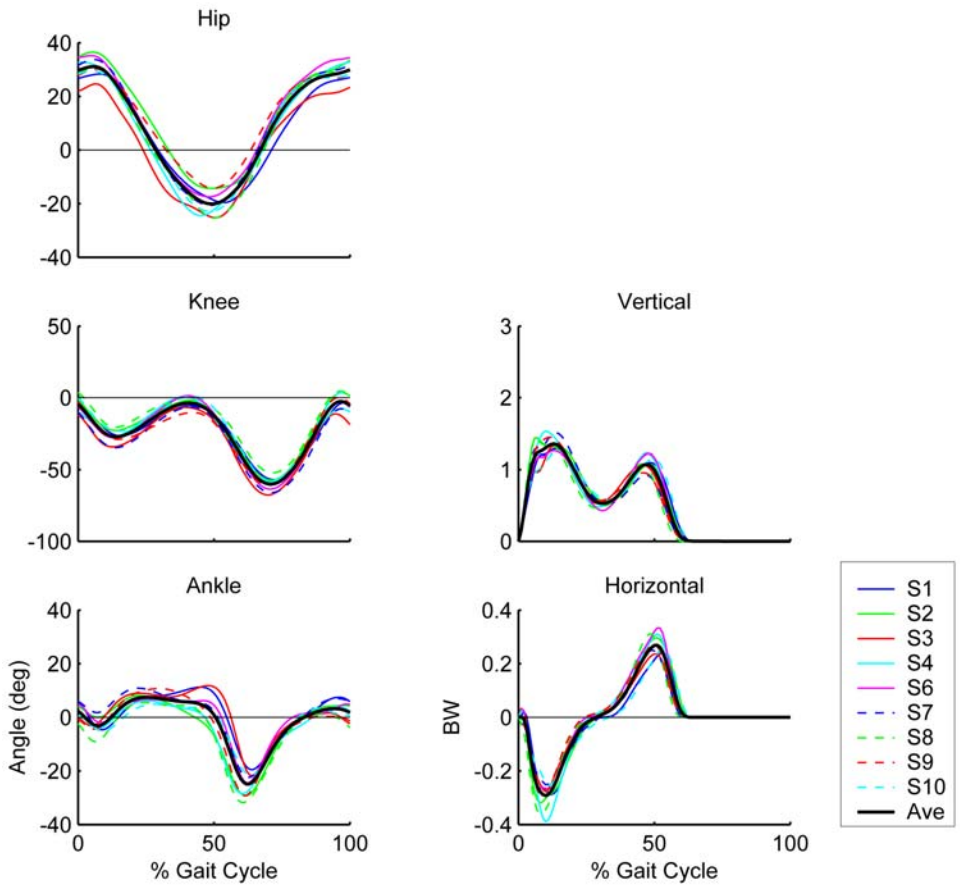

Fig. A2.3: Ensemble and group average kinematic and GRF data in W100

Hip, knee and ankle joint angles and vertical and horizontal ground reaction forces in walking at 100% PTS in nine subjects (S1-S10, except S5) and group average data (thick solid line). S5 was excluded due to data corruption.

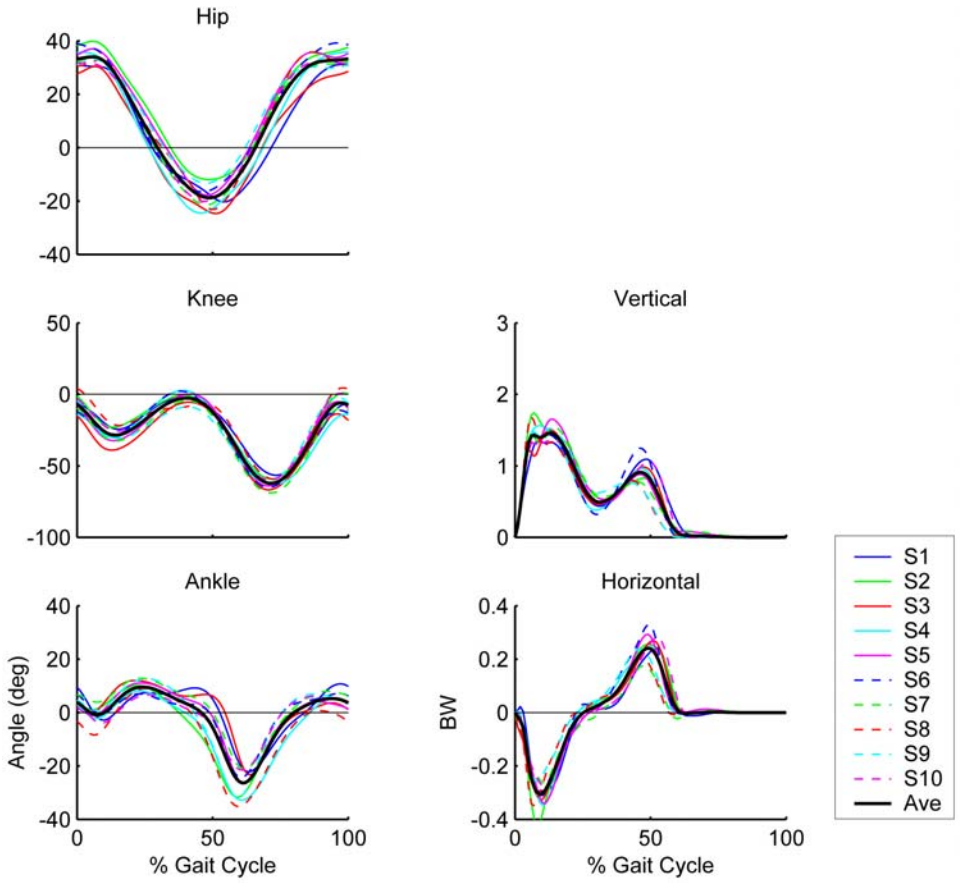

Fig. A2.4: Ensemble and group average kinematic and GRF data in W120

Hip, knee and ankle joint angles and vertical and horizontal ground reaction forces in walking at 120% PTS in ten subjects (S1-S10) and group average data (thick solid line).

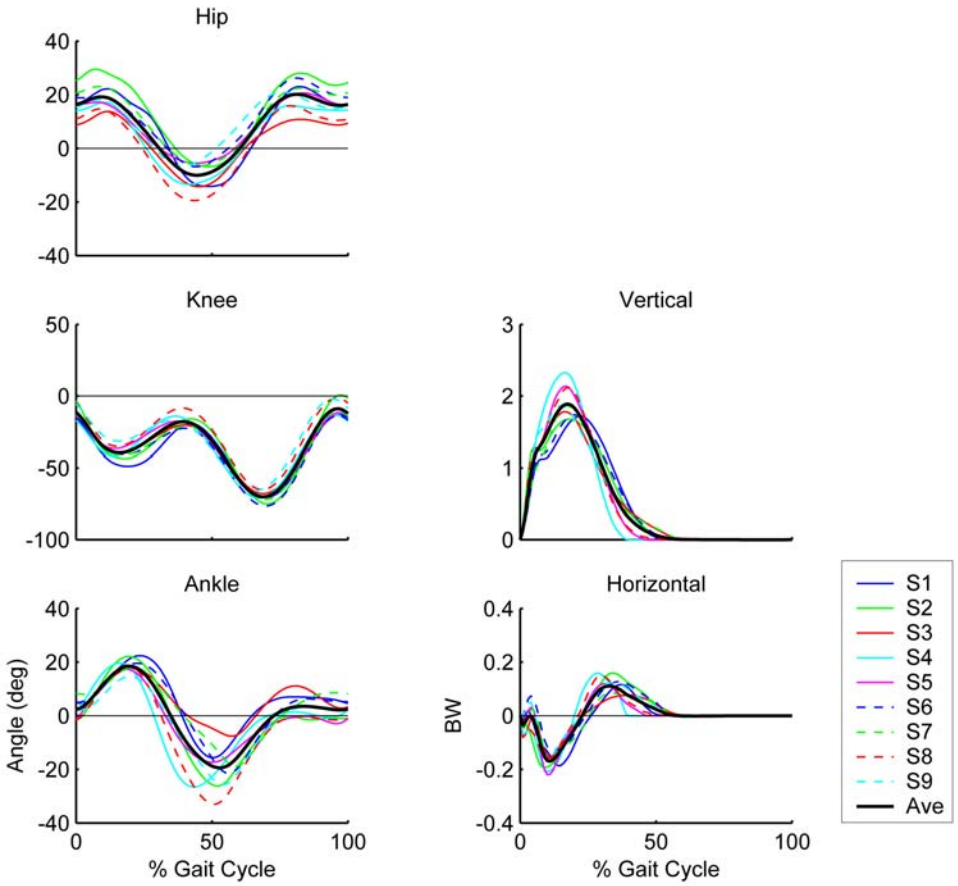

Fig. A2.5: Ensemble and group average kinematic and GRF data in R80

Hip, knee and ankle joint angles and vertical and horizontal ground reaction forces in running at 80% PTS in nine subjects (S1-S9) and group average data (thick solid line). S10 was excluded due to data corruption.

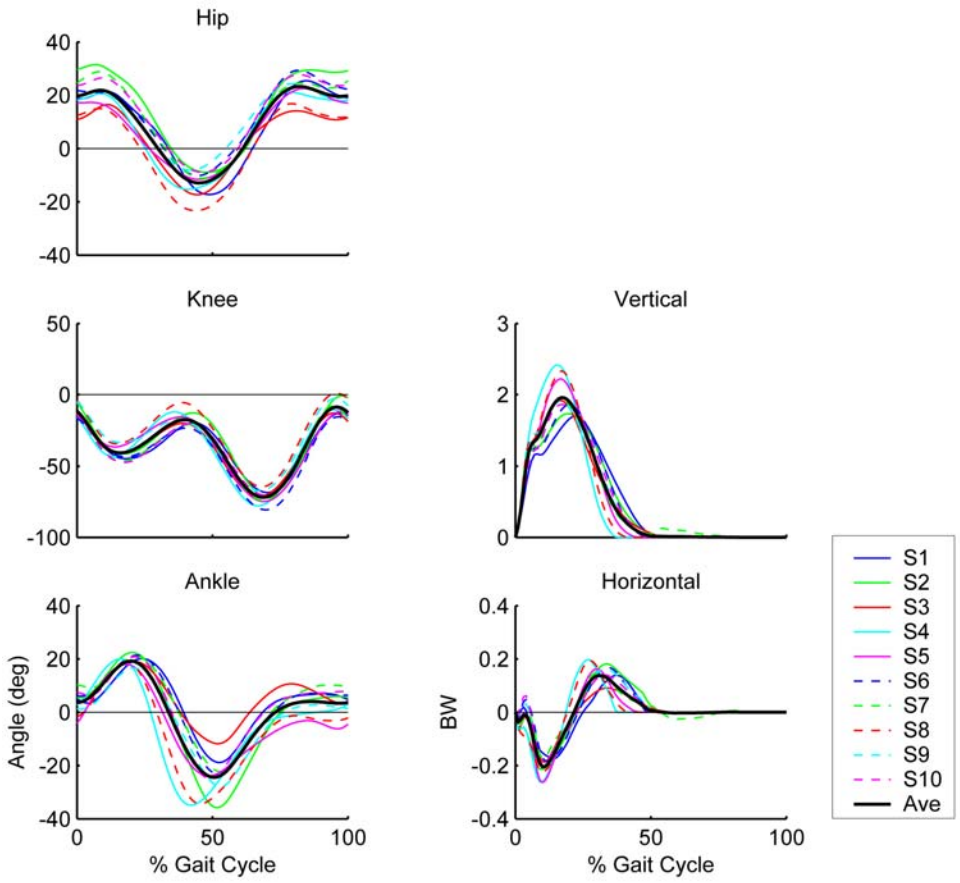

Fig. A2.6: Ensemble and group average kinematic and GRF data in R100

Hip, knee and ankle joint angles and vertical and horizontal ground reaction forces in running at 100% PTS in ten subjects (S1-S10) and group average data (thick solid line).

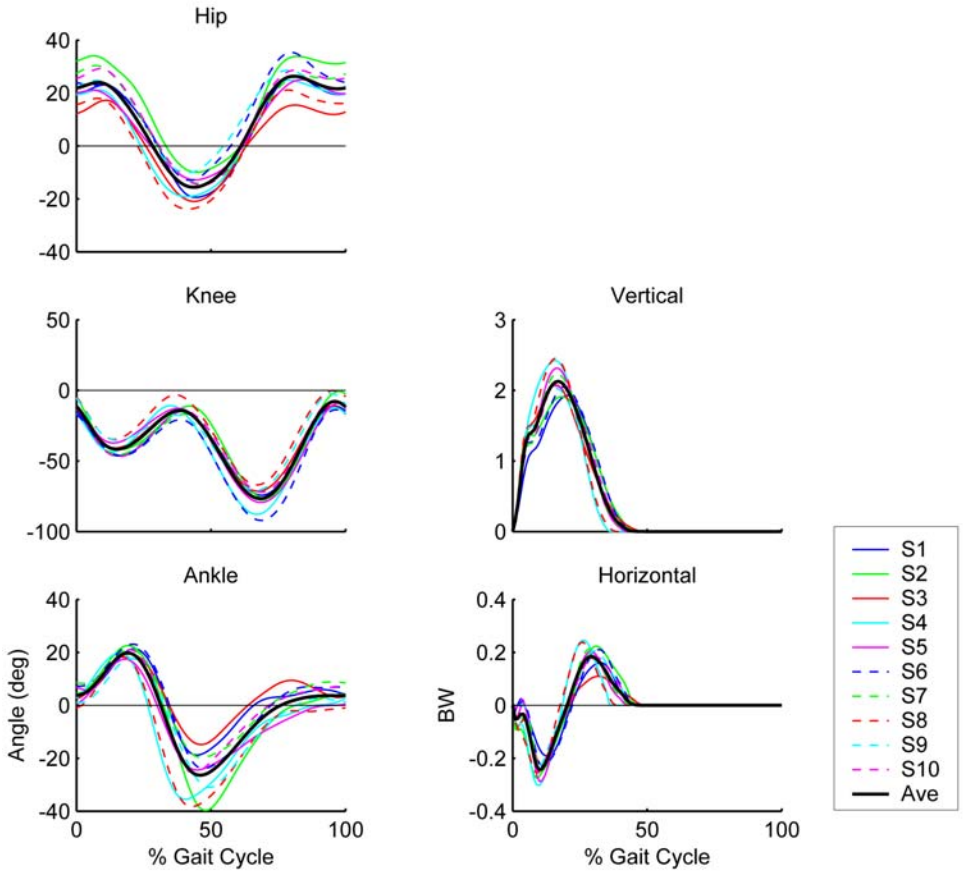

Fig. A2.7: Ensemble and group average kinematic and GRF data in R120

Hip, knee and ankle joint angles and vertical and horizontal ground reaction forces in running at 120% PTS in ten subjects (S1-S10) and group average data (thick solid line).

Appendix 3

(Sensitivity analysis: Running)

The tracking optimization in the present study generated running simulations that closely emulated the group-averaged kinematic data. However, the tracking errors in the ground reaction forces (GRFs) were often greater than the kinematic errors. The GRF tracking could be improved by increasing the weighting of the GRFs in the cost function, although the kinematic errors would subsequently increase. Since the muscle kinematics were an important focus of the present study, we chose to closely track the kinematic data at the expense of increased GRF tracking errors. To assess whether this choice would affect our results, we performed a sensitivity analysis to examine the influence of GRF tracking accuracy on the interpretation of muscle function (i.e., contributions to segment power and muscle-induced accelerations). Two running simulations at the preferred transition speed with different GRF tracking accuracy were analyzed. One was the original simulation (presented in Chapter 2) with better kinematic tracking (Fig. A3.1: Simulation 1), and the other yielded better GRF tracking results with larger deviations in joint angles (Fig. A3.1: Simulation2). The results of the sensitivity analysis on the muscle contributions to segment power and muscle-induced accelerations showed that the qualitative function of each muscle remained unaltered (Figs. A3.2-3).

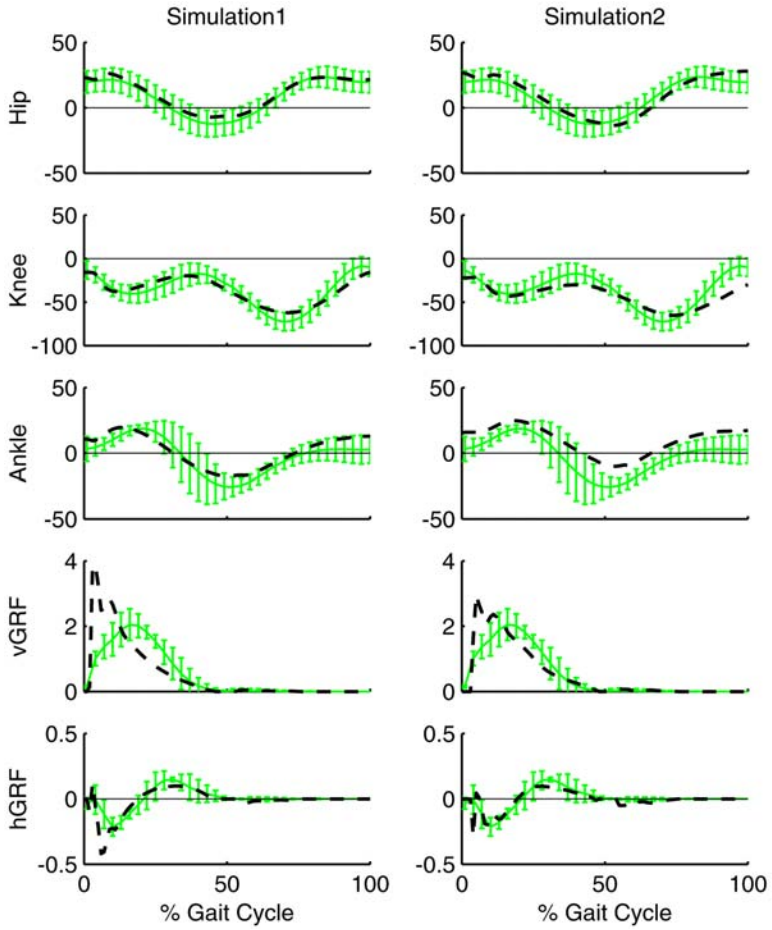

Fig. A3.1: Tracking results of running at the preferred transition speed

Hip, knee and ankle joint angles (units: degrees) and vertical (vGRF) and horizontal (hGRF) ground reaction forces (units: normalized to body weight) in two running simulations (dashed line) and experimental data (solid line, average ± 2 S.D.) at the preferred transition speed. Positive angles are flexion, extension and dorsiflexion in the hip, knee and ankle joints, respectively. Simulation1 is the original running simulation (identical to Fig.2.2: Running). Simulation2 has better GRF tracking results at the expense of larger deviations in joint angles, compared to Simulation1.

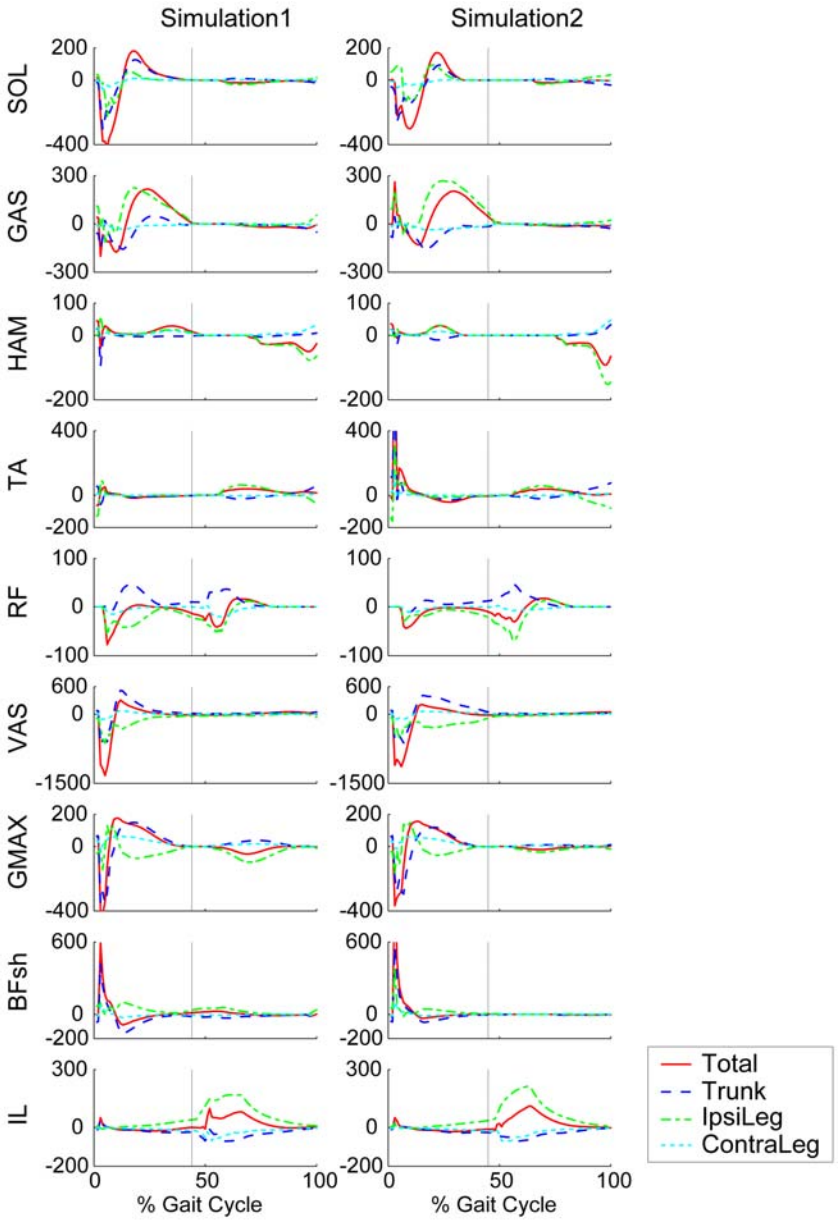

Fig. A3.2: Segment power in two running simulations

Distribution of muscle mechanical power (units: watts) to the trunk (Trunk), ipsilateral leg (IpsiLeg) and contralateral leg (ContraLeg) during running at the preferred transition speed over the gait cycle (right foot-strike to right foot-strike). The vertical lines indicate toe-off. Simulation1 is the original running simulation. Simulation2 has better GRF tracking results at the expense of larger deviations in joint angles, compared to Simulation1 (see Fig. A3.1).

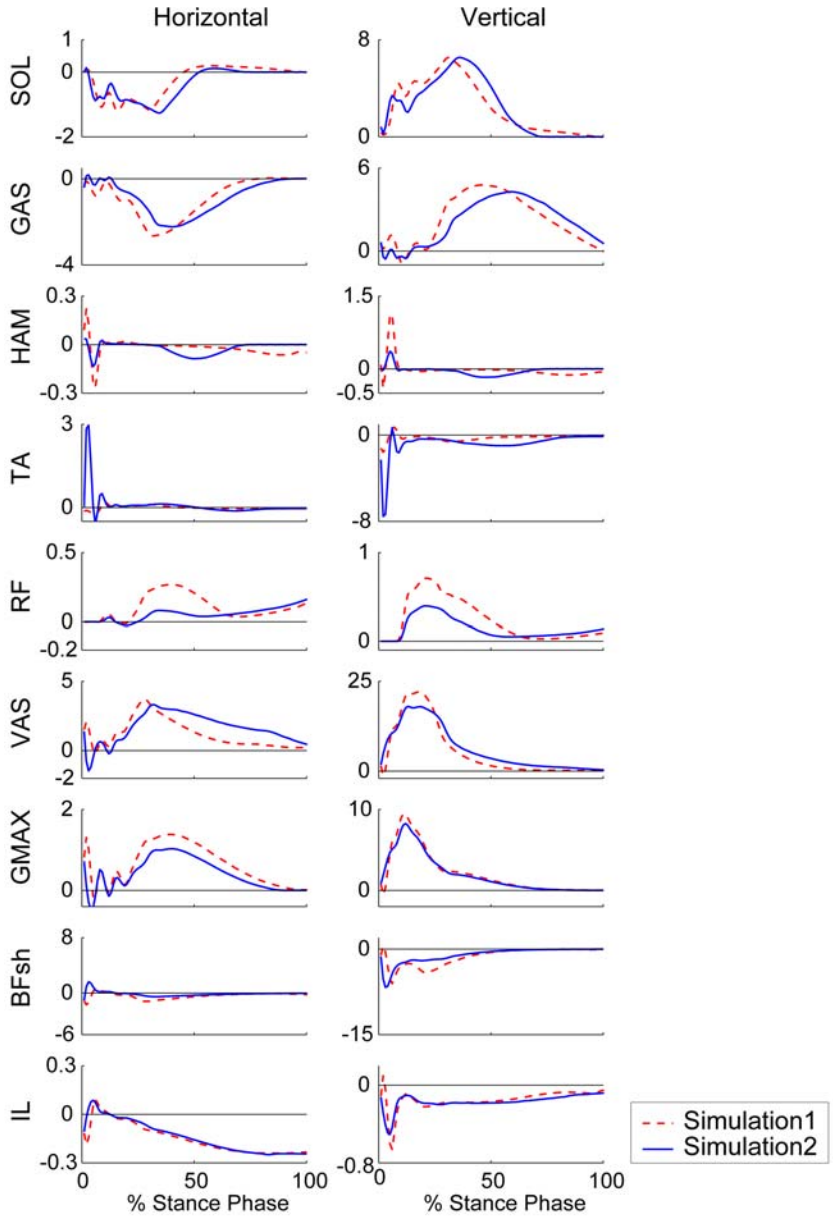

Fig. A3.3: Muscle-induced accelerations in two running simulations

Trunk horizontal and vertical muscle-induced accelerations (units: m/s^2) during stance in the original running simulation (Simulation1: dashed line) and a different running simulation (Simulation2: solid line, see Fig. A3.1). The stance phase is defined from foot-strike to toe-off of the ipsilateral leg. Simulation2 has better GRF tracking results at the expense of larger deviations in joint angles, compared to Simulation1.

Appendix 4

(Snapshots of walking and running at the preferred transition speed)

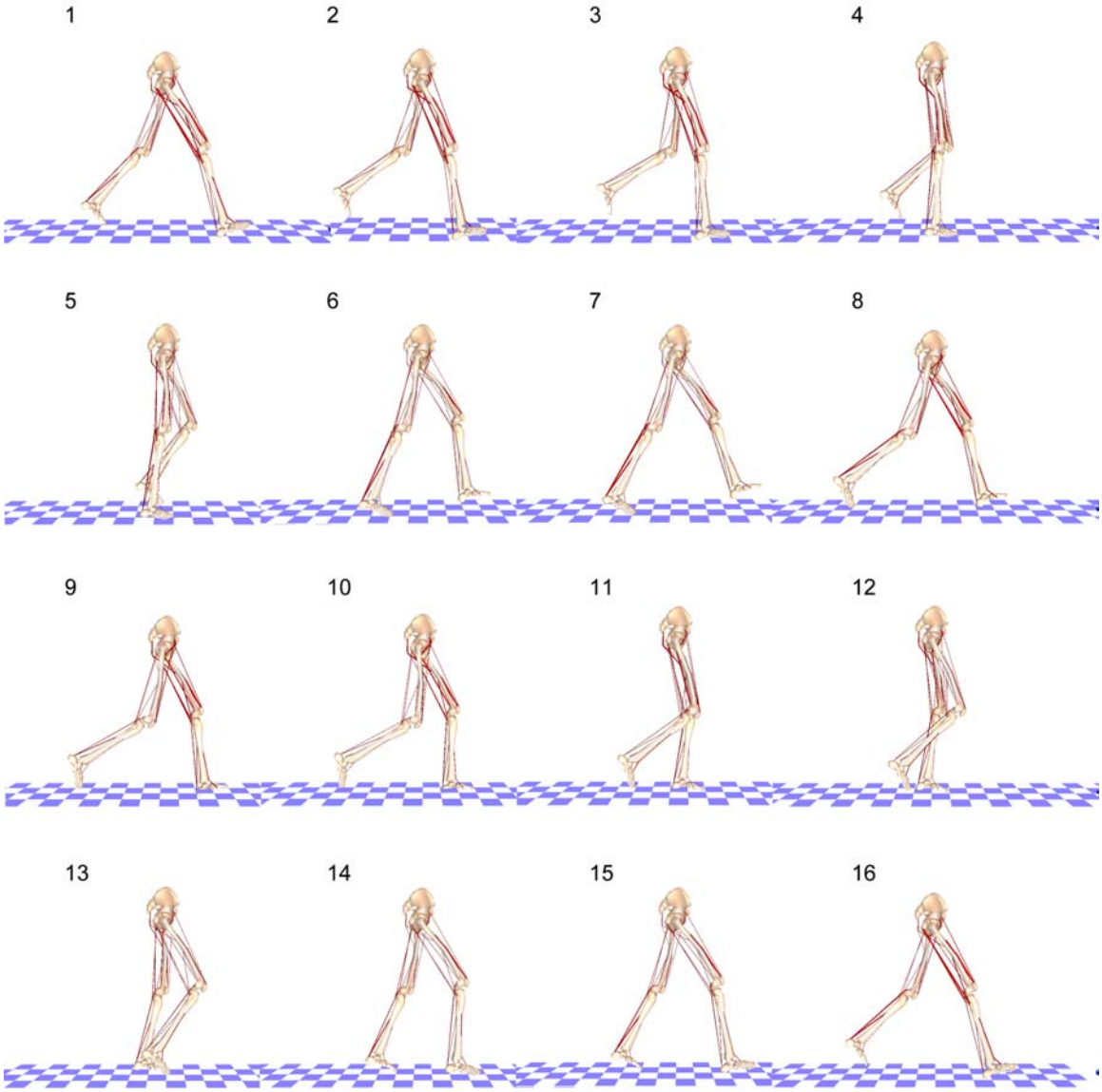

Fig. A4.1: Gait pattern of the walking simulation at the preferred transition speed

The figures are from right heel-strike (frame 1) to the right heel-strike (frame 16).

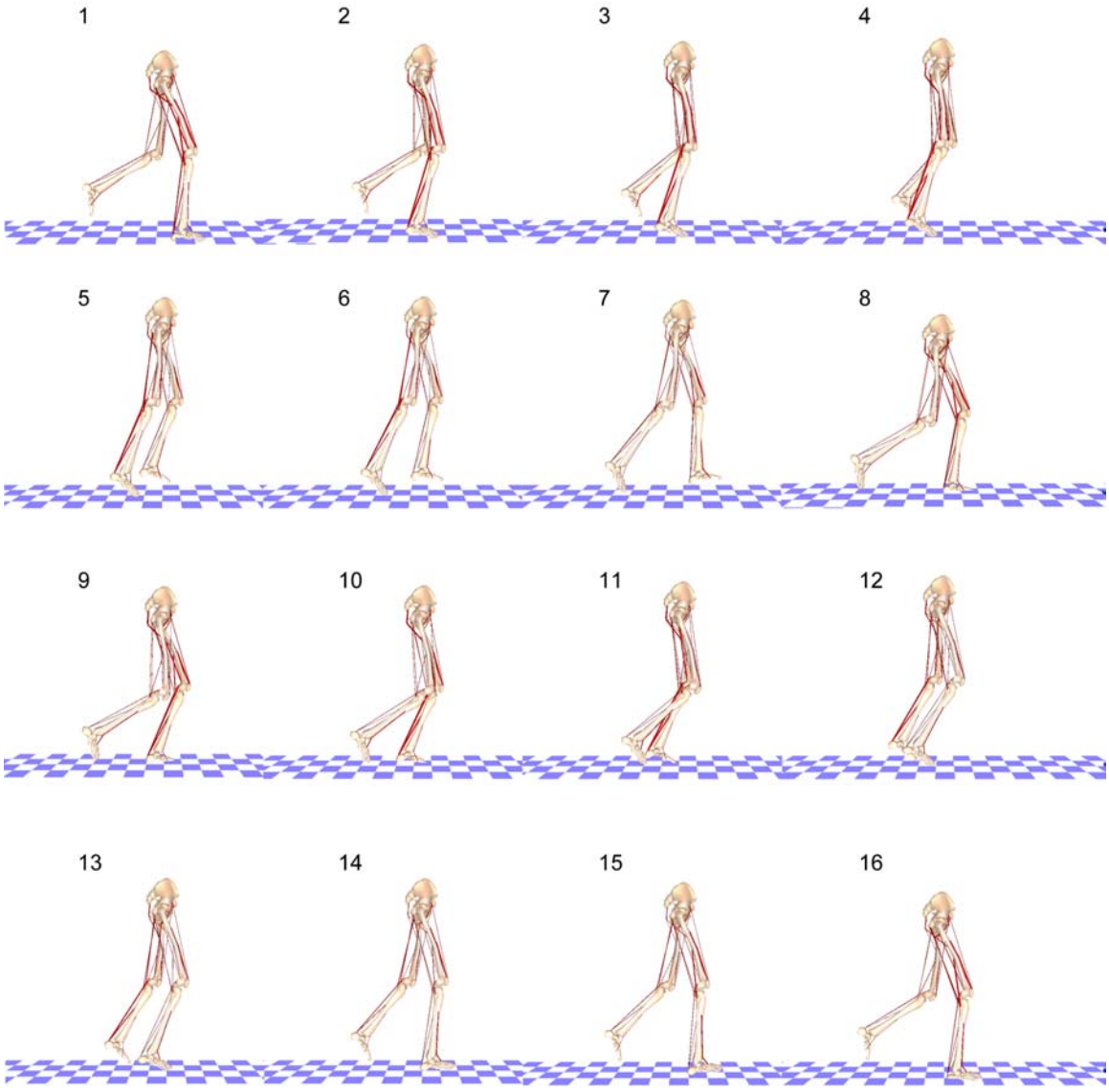

Fig. A4.2: Gait pattern of the running simulation at the preferred transition speed

The figures are from right foot-strike (frame 1) to the right foot-strike (frame 16).

Bibliography

Alexander, R. M. (1984). Walking and running. American Scientist. **72:** 348-354.

Alexander, R. M. (1988). Springs as energy stores: running. Elastic mechanisms in animal movement, Cambridge University Press**:** 30-50.

Alexander, R. M. and Bennet-Clark, H. C., 1977. Storage of elastic strain energy in muscle and other tissues. Nature **265**, 114-7.

Anderson, F. C. (1999). A dynamic optimization solution for a complete cycle of normal gait. Department of Mechanical Engineering. Austin, TX, University of Texas at Austin**:** 440.

Anderson, F. C. and Pandy, M. G., 2003. Individual muscle contributions to support in normal walking. Gait Posture **17**, 159-69.

Andersson, E. A., Nilsson, J. and Thorstensson, A., 1997. Intramuscular EMG from the hip flexor muscles during human locomotion. Acta Physiol Scand **161**, 361-70.

Antonsson, E. K. and Mann, R. W., 1985. The frequency content of gait. J Biomech **18**, 39-47.

Belli, A., Kyrolainen, H. and Komi, P. V., 2002. Moment and power of lower limb joints in running. Int J Sports Med **23**, 136-41.

Biewener, A. A., Konieczynski, D. D. and Baudinette, R. V., 1998. In vivo muscle force-length behavior during steady-speed hopping in tammar wallabies. J Exp Biol **201 (Pt 11)**, 1681-94.

Biewener, A. A. and Roberts, T. J., 2000. Muscle and tendon contributions to force, work, and elastic energy savings: a comparative perspective. Exerc Sport Sci Rev **28**, 99-107.

Brandell, B. R. (1973). An analysis of muscle coordination in walking and running gaits. Medicine and Sport: Biomechanics III. A. Cerquiglini, A. Venerando and J. Wartenweiler. Basel, Switzerland, Karger. **8:** 278-287.

Brisswalter, J. and Mottet, D., 1996. Energy cost and stride duration variability at preferred transition gait speed between walking and running. Can. J. Appl. Physiol. **21**, 471-480.

Caldwell, G. E. and Forrester, L. W., 1992. Estimates of mechanical work and energy transfers: demonstration of a rigid body power model of the recovery leg in gait. Med Sci Sports Exerc **24**, 1396-412.

Carhart, M. R. (2000). Biomechanical analysis of compensatory stepping: implications for paraplegics standing via FNS. Department of Bioengineering. Tempa, AZ, Arizona State University**:** 321.

Cavagna, G. A. and Kaneko, M., 1977. Mechanical work and efficiency in level walking and running. J Physiol **268**, 467--81.

Cavagna, G. A. and Margaria, R., 1966. Mechanics of walking. J. Appl. Physiol. **21**, 271-278.

Cavagna, G. A., Thys, H. and Zamboni, A., 1976. The sources of external work in level walking and running. J Physiol **262**, 639-57.

Curtin, N. A. and Davies, R. E., 1975. Very high tension with very little ATP breakdown by active skeletal muscle. J Mechanochem Cell Motil **3**, 147-54.
Davy, D. T. and Audu, M. L., 1987. A dynamic optimization technique for predicting muscle forces in the swing phase of gait. J Biomech **20**, 187-201.
Delp, S. L. (1990). Surgery simulation: a computer graphics system to analyze and design musculoskeletal reconstructions of the lower limb. Department of Mechanical Engineering. Stanford, CA, Stanford University.
Diedrich, F. J. and Warren, W. H., Jr., 1995. Why change gaits? Dynamics of the walk-run transition. J Exp Psychol Hum Percept Perform **21**, 183-202.
Fregly, B. J. and Zajac, F. E., 1996. A state-space analysis of mechanical energy generation, absorption, and transfer during pedaling. J.Biomech. **29**, 81-90.
Fukunaga, T., Kawakami, Y., Kubo, K. and Kanehisa, H., 2002. Muscle and tendon interaction during human movements. Exerc Sport Sci Rev **30**, 106-10.
Fukunaga, T., Kubo, K., Kawakami, Y., Fukashiro, S., Kanehisa, H. and Maganaris, C. N., 2001. In vivo behaviour of human muscle tendon during walking. Proc R Soc Lond B Biol Sci **268**, 229-33.
Goffe, W. L., Ferrier, G. D. and Rogers, J., 1994. Global optimization of statistical functions with simulated annealing. J. Econometrics **60**, 65-99.
Gonzalez, R. V., Hutchins, E. L., Barr, R. E. and Abraham, L. D., 1996. Development and evaluation of a musculoskeletal model of the elbow joint complex. J Biomech Eng **118**, 32-40.
Grillner, S., Halbertsma, J., Nilsson, L. and Thorstensson, A., 1979. The adaptation to speed in human locomotion. Brain Research **165**, 177-182.
Hanna, A., Abernethy, B., Neal, R. J. and Burgess-Limerick, R. (2000). Triggers for the transition between human walking and running. Energetics of Human Activity. W. A. Sparrow. Chicago, Human Kinerics**:** 124-164.
Hinrichs, R. N. (1990). Upper extremity function in distance running. Biomechanics of distance running. P. R. Cavanagh. Champaign, IL, Human Kinetics Publishers, Inc.**:** 107-133.
Hof, A. L. (1990). Effects of muscle elasticity in walking and running. Multiple muscle systems: Biomechanics and movement organization. J. M. Winters and S. L.-Y. Woo. New York, Springer-Verlag, Inc.**:** 591-607.
Hof, A. L., Van Zandwijk, J. P. and Bobbert, M. F., 2002. Mechanics of human triceps surae muscle in walking, running and jumping. Acta Physiol Scand **174**, 17-30.
Hreljac, A., 1993a. Preferred and energetically optimal gait transition speeds in human locomotion. Med Sci Sports Exerc **25**, 1158-62.
Hreljac, A., 1993b. Determinants of the gait transition speed during human locomotion: kinetic factors. Gait & Posture **1**, 217-223.
Hreljac, A., 1995a. Determinants of the gait transition speed during human locomotion: kinematic factors. Journal of Biomechanics **28**, 669-677.
Hreljac, A., 1995b. Effects of physical characteristics on the gait transition speed during human locomotion. Human Movement Science **14**, 205-216.
Hreljac, A., Arate, A., Ferber, R., Mercer, J. A. and Row, B. S., 2001. An electromyographical analysis of the role of dorsiflexors on the gait transition during human locomotion. Journal of Applied Biomechanics **17**, 287-296.

Kane, T. R. and Levinson, D. A., 1985. Dynamics: Theory and Applications. New York, McGraw-Hill.
Kawakami, Y., Ichinose, Y. and Fukunaga, T., 1998. Architectural and functional features of human triceps surae muscles during contraction. J Appl Physiol **85**, 398-404.
Ker, R. F., Bennett, M. B., Bibby, S. R., Kester, R. C. and Alexander, R. M., 1987. The spring in the arch of the human foot. Nature **325**, 147-9.
Komi, P. V., Fukashiro, S. and Jarvinen, M., 1992. Biomechanical loading of Achilles tendon during normal locomotion. Clin Sports Med **11**, 521-31.
Kram, R., Domingo, A. and Ferris, D. P., 1997. Effect of reduced gravity on the preferred walk-run transition speed. Journal of Experimental Biology **200**, 821-826.
Kram, R. and Taylor, C. R., 1990. Energetics of running: a new perspective. Nature **346**, 265-7.
Kyrolainen, H., Finni, T., Avela, J. and Komi, P. V., 2003. Neuromuscular behaviour of the triceps surae muscle-tendon complex during running and jumping. Int J Sports Med **24**, 153-5.
Kyrolainen, H., Komi, P. V. and Belli, A., 1999. Changes in muscle activity patterns and kinetics with increasing running speed. Journal of Strength and Conditioning Research **13**, 400-406.
Li, L., et al., 1999. Coordination patterns of walking and running at similar speed and stride frequency. Human Movement Science **18**, 67-85.
Liu, W. and Nigg, B. M., 2000. A mechanical model to determine the influence of masses and mass distribution on the impact force during running. J Biomech **33**, 219-24.
Mann, R. and Sprague, P., 1980. A kinetic analysis of the ground leg during sprint running. Res Q Exerc Sport **51**, 334-48.
Mann, R. A., Moran, G. T. and Dougherty, S. E., 1986. Comparative electromyography of the lower extremity in jogging, running, and sprinting. Am J Sports Med **14**, 501-10.
Margaria, R., Cerretelli, P., Aghemo, P. and Sassi, G., 1963. Energy cost of running. J. Appl. Physiol **18**, 367-370.
Marsh, R. L., Ellerby, D. J., Carr, J. A., Henry, H. T. and Buchanan, C. I., 2004. Partitioning the energetics of walking and running: swinging the limbs is expensive. Science **303**, 80-3.
Mercier, J., Le Gallais, D., Durand, M., Goudal, C., Micallef, J. P. and Prefaut, C., 1994. Energy expenditure and cardiorespiratory responses at the transition between walking and running. Eur J Appl Physiol **69**, 525-529.
Minetti, A. E., Ardigo, L. P. and Saibene, F., 1994. The transition between walking and running in humans: metabolic and mechanical aspects at different gradients. Acta Physiol Scand **150**, 315-23.
Minetti, A. E., Capelli, C., Zamparo, P., di Prampero, P. E. and Saibene, F., 1995. Effects of stride frequency on mechanical power and energy expenditure of walking. Med Sci Sports Exerc **27**, 1194-202.
Narici, M. V., Binzoni, T., Hiltbrand, E., Fasel, J., Terrier, F. and Cerretelli, P., 1996. In vivo human gastrocnemius architecture with changing joint angle at rest and during graded isometric contraction. J Physiol **496 (Pt 1)**, 287-97.

Neptune, R. R. and Hull, M. L., 1998. Evaluation of performance criteria for simulation of submaximal steady-state cycling using a forward dynamic model. J Biomech Eng **120**, 334-41.
Neptune, R. R., Kautz, S. A. and Zajac, F. E., 2001. Contributions of the individual ankle plantar flexors to support, forward progression and swing initiation during walking. J Biomech **34**, 1387-98.
Neptune, R. R. and Sasaki, K. (2004). Insight from ground reaction forces into the preferred gait transition speed. 9th Annual Meeting of the Gait and Clinical Movement Analysis Society, Lexington, Kentucky.
Neptune, R. R. and van den Bogert, A. J., 1998. Standard mechanical energy analyses do not correlate with muscle work in cycling. J Biomech **31**, 239-45.
Neptune, R. R., Wright, I. C. and van den Bogert, A. J., 2000. A method for numerical simulation of single limb ground contact events: application to heel-toe running. Comp Meth Biomech Biomed Eng **3**, 321-334.
Neptune, R. R., Zajac, F. E. and Kautz, S. A., 2004a. Muscle force redistributes segmental power for body progression during walking. Gait Posture **19**, 194-205.
Neptune, R. R., Zajac, F. E. and Kautz, S. A., 2004b. Muscle mechanical work requirements during normal walking: the energetic cost of raising the body's center-of-mass is significant. J Biomech **37**, 817-25.
Nilsson, J. and Thorstensson, A., 1989. Ground reaction forces at different speeds of human walking and running. Acta Physiol Scand **136**, 217-27.
Nilsson, J., Thorstensson, A. and Halbertsma, J., 1985. Changes in leg movements and muscle activity with speed of locomotion and mode of progression in humans. Acta Physiologica Scandinavica **123**, 457-75.
Novacheck, T. F., 1998. Review paper: The biomechanics of running. Gait and Posture **7**, 77-95.
Ounpuu, S., 1990. The biomechanics of running: a kinematic and kinetic analysis. Instructional course lectures **39**, 305-18.
Perotto, A., 1994. Anatomical guide for the electromyographer: the limbs and trunk. Springfield, IL, Charles C Thomas Publisher.
Prilutsky, B. I. and Gregor, R. J., 2001. Swing- and support-related muscle actions diffrentially trigger human walk-run and run-walk transitions. Journal of Experimental Biology **204**, 2277-2287.
Raasch, C. C., Zajac, F. E., Ma, B. and Levine, W. S., 1997. Muscle coordination of maximum-speed pedaling. J Biomech **30**, 595-602.
Raynor, A. J., Yi, C. J., Abernethy, B. and Jong, Q. J., 2002. Are transitions in human gait determined by mechanical, kinetic or energetic factors? Hum Mov Sci **21**, 785-805.
Reber, L., Perry, J. and Pink, M., 1993. Muscular control of the ankle in running. Am J Sports Med **21**, 805-10; discussion 810.
Roberts, T. J., 2002. The integrated function of muscles and tendons during locomotion. Comp Biochem Physiol A Mol Integr Physiol **133**, 1087-99.
Roberts, T. J., Marsh, R. L., Weyand, P. G. and Taylor, C. R., 1997. Muscular force in running turkeys: the economy of minimizing work. Science **275**, 1113-5.

Schache, A. G., Bennell, K. L., Blanch, P. D. and Wrigley, T. V., 1999. The coordinated movement of the lumbo-pelvic-hip complex during running: a literature review. Gait Posture **10**, 30-47.

Seyfarth, A., Geyer, H., Gunther, M. and Blickhan, R., 2002. A movement criterion for running. J Biomech **35**, 649-55.

Simonsen, E. B., Thomsen, L. and Klausen, K., 1985. Activity of mono- and biarticular leg muscles during sprint running. Eur J Appl Physiol Occup Physiol **54**, 524-32.

Simpson, K. J. and Bates, B. T., 1990. The effects of running speed on lower extremity joint moments generated during the support phase. International Journal of Sport Biomechanics **6**, 309-324.

Sparrow, W. A., Hughes, K. M., Russell, A. P. and Le Rossignol, P. F. (2000). Movement economy, preferred modes, and pacing. Energetics of Human Activity. W. A. Sparrow. Chicago, Human Kinerics**:** 96-123.

Stefanyshyn, D. J. and Nigg, B. M., 1997. Mechanical energy contribution of the metatarsophalangeal joint to running and sprinting. J Biomech **30**, 1081-5.

Swanson, S. C. and Caldwell, G. E., 2000. An integrated biomechanical analysis of high speed incline and level treadmill running. Med Sci Sports Exerc **32**, 1146-55.

Taylor, C. R., Heglund, N. C., McMahon, T. A. and Looney, T. R., 1980. Energetic cost of generating muscular force during running. J Exp Biol **86**, 9-18.

Thelen, D. G., Anderson, F. C. and Delp, S. L., 2003. Generating dynamic simulations of movement using computed muscle control. J Biomech **36**, 321-8.

Thorstensson, A. and Roberthson, H., 1987. Adaptations to changing speed in human locomotion: speed of transition between walking and running. Acta Physiol Scand **131**, 211-4.

Tseh, W., Bennett, J., Caputo, J. L. and Morgan, D. W., 2002. Comparison between preferred and energetically optimal transition speeds in adolescents. Eur J Appl Physiol **88**, 117-21.

Wickiewicz, T. L., Roy, R. R., Powell, P. L. and Edgerton, V. R., 1983. Muscle architecture of the human lower limb. Clin Orthop, 275-83.

Winter, D. A., 1979. A new definition of mechanical work done in human movement. J Appl Physiol **46**, 79-83.

Winter, D. A., 1990. Biomechanics and motor control of human movement. New York, John Wiley & Sons, Inc.

Yamaguchi, G. T., Moran, D. W. and Si, J., 1995. A computationally efficient method for solving the redundant problem in biomechanics. J Biomech **28**, 999-1005.

Yamaguchi, G. T. and Zajac, F. E., 1989. A planar model of the knee joint to characterize the knee extensor mechanism. J Biomech **22**, 1-10.

Zajac, F. E., 1989. Muscle and tendon: properties, models, scaling, and application to biomechanics and motor control. Crit.Rev.Biomed.Eng. **17**, 359-411.

Zajac, F. E., Neptune, R. R. and Kautz, S. A., 2003. Biomechanics and muscle coordination of human walking: part II: lessons from dynamical simulations and clinical implications. Gait Posture **17**, 1-17.

Vita

Kotaro Sasaki was born in Akashi City, Hyogo, Japan on November 15, 1966, the son of Mizuho and Sadao Sasaki. In April of 1985 he entered Osaka University in Osaka, Japan, where he majored in biophysical engineering and received a Bachelor of Science in 1989. In April of 1989 he was employed as an engineer with the Shimadzu Corporation in Kyoto, Japan. In August of 1995, he entered the Department of Kinesiology of the Graduate School at The University of Texas at Austin. He received a Master of Arts in 1997. In August of 1998, he entered the Department of Mechanical Engineering of the Graduate School at The University of Texas at Austin.

Permanent address: 17-2 Asagiri Yamatecho, Akashi, Hyogo 673-0853, Japan

This dissertation was typed by Kotaro Sasaki.